Original Article

MOLECULAR METABOLISM

RIPK1 and RIPK3 regulate TNFα-induced β-cell death in concert with caspase activity

Christopher J. Contreras [1], Noyonika Mukherjee [2], Renato C.S. Branco [3], Li Lin [3], Meghan F. Hogan [4], Erica P. Cai [3], Andrew A. Oberst [5], Steven E. Kahn [4], Andrew T. Templin [1,2,3,6,*]

ABSTRACT

Objective: Type 1 diabetes (T1D) is characterized by autoimmune-associated β-cell loss, insulin insufficiency, and hyperglycemia. Although TNFα signaling is associated with β-cell loss and hyperglycemia in non-obese diabetic mice and human T1D, the molecular mechanisms of β-cell TNF receptor signaling have not been fully characterized. Based on work in other cell types, we hypothesized that receptor interacting protein kinase 1 (RIPK1) and receptor interacting protein kinase 3 (RIPK3) regulate TNFα-induced β-cell death in concert with caspase activity.

Methods: We evaluated TNFα-induced cell death, caspase activity, and TNF receptor pathway molecule expression in immortalized NIT-1 and INS-1 β-cell lines and primary mouse islet cells *in vitro*. Our studies utilized genetic and small molecule approaches to alter RIPK1 and RIPK3 expression and caspase activity to interrogate mechanisms of TNFα-induced β-cell death. We used the β-cell toxin streptozotocin (STZ) to determine the susceptibility of $Ripk3^{+/+}$ and $Ripk3^{-/-}$ mice to hyperglycemia *in vivo*.

Results: Expression of TNF receptor signaling molecules including RIPK1 and RIPK3 was identified in NIT-1 and INS-1 β cells and isolated mouse islets at the mRNA and protein levels. TNFα treatment increased NIT-1 and INS-1 cell death and caspase activity after 24—48 h, and BV6, a small molecule inhibitor of inhibitor of apoptosis proteins (IAPs) amplified this TNFα-induced cell death. RIPK1 deficient NIT-1 cells were protected from TNFα- and BV6-induced cell death and caspase activation. Interestingly, small molecule inhibition of caspases with zVAD-fmk (zVAD) did not prevent TNFα-induced cell death in either NIT-1 or INS-1 cells. This caspase-independent cell death was increased by BV6 treatment and decreased in RIPK1 deficient NIT-1 cells. RIPK3 deficient NIT-1 cells and RIPK3 kinase inhibitor treated INS-1 cells were protected from TNFα+zVAD-induced cell death, whereas RIPK3 overexpression increased INS-1 cell death and promoted RIPK3 and MLKL interaction under TNFα+zVAD treatment. In mouse islet cells, BV6 or zVAD treatment promoted TNFα-induced cell death, and TNFα+zVAD-induced cell death was blocked by RIPK3 inhibition and in $Ripk3^{-/-}$ islet cells *in vitro*. $Ripk3^{-/-}$ mice were also protected from STZ-induced hyperglycemia and glucose intolerance *in vivo*.

Conclusions: RIPK1 and RIPK3 regulate TNFα-induced β-cell death in concert with caspase activity in immortalized and primary islet β cells. TNF receptor signaling molecules such as RIPK1 and RIPK3 may represent novel therapeutic targets to promote β-cell survival and glucose homeostasis in T1D.

Keywords RIPK1; RIPK3; β-cell death; Type 1 diabetes; TNFα; Caspase

1. INTRODUCTION

TNFα is a proinflammatory cytokine associated with β-cell loss, insulin insufficiency and hyperglycemia in the pathogenesis of type 1 diabetes (T1D) [1—5]. Previous studies found that TNFα elicits β-cell death in NIT-1 and MIN6 β-cell lines *in vitro*, with Fas-associated death domain (FADD) promoting this process [6] and NFκB signaling inhibiting it [7]. Other studies failed to observe TNFα-induced β-cell death [8] or observed it only in the presence of cycloheximide [9]. Although primary islet β cells are less prone to TNFα-induced cell death *in vitro*, TNFα and IFNγ cotreatment strongly elicits primary β-cell death, which Irawaty and colleagues found to be caspase-independent [6,10]. *In vivo*, overexpression of TNFα in β cells accelerates the onset of hyperglycemia in the non-obese diabetic (NOD) mouse model of T1D [3], while either loss of TNF receptor 1 (TNFR1) [4] or treatment with an anti-TNFα antibody [11] protects NOD mice from hyperglycemia. In humans, etanercept, a TNFα neutralizing antibody was shown to promote glucose homeostasis and β-cell function in a pilot study of 18 individuals with newly diagnosed T1D [12], and more recently, golimumab, an anti-TNFα monoclonal antibody, was shown to preserve β-cell function in a cohort of 84 children and young adults with new-onset T1D [5], revealing the importance of this pathway in human disease. Although these studies established that TNFα promotes hyperglycemia in T1D, the role of TNFα-mediated β-cell loss in this

[1]Division of Endocrinology, Department of Medicine, Roudebush VA Medical Center and Indiana University School of Medicine, Indianapolis, IN, USA [2]Department of Biochemistry and Molecular Biology, Indiana University School of Medicine, Indianapolis, IN, USA [3]Lilly Diabetes Center of Excellence, Indiana Biosciences Research Institute, Indianapolis, IN, USA [4]Division of Metabolism, Endocrinology and Nutrition, Department of Medicine, VA Puget Sound Health Care System and University of Washington, Seattle, WA, USA [5]Department of Immunology, University of Washington, Seattle, WA, USA [6]Center for Diabetes and Metabolic Diseases, Indiana University School of Medicine, Indianapolis, IN, USA

*Corresponding author. 1210 Waterway Blvd., Ste. 2000, Indianapolis, IN, USA, 46202. E-mail: templin@iu.edu (A.T. Templin).

Received June 22, 2022 • Revision received August 16, 2022 • Accepted August 19, 2022 • Available online 24 August 2022

https://doi.org/10.1016/j.molmet.2022.101582

process remains poorly understood. As such, studies to characterize the mechanisms of β-cell TNF receptor signaling may lead to novel approaches to protect β cells and diminish hyperglycemia in T1D.

Although studies of TNFα-induced β-cell death have focused on apoptosis [2,13], in other cell types TNFα can elicit a distinct mechanism of caspase-independent programmed cell death termed necroptosis [14,15]. In contrast to apoptosis, necroptosis is an inflammatory and immunogenic form of lytic cell death that occurs when caspases are inactivated [16,17], leading to release of damage-associated molecular patterns and immune responses [17,18]. Following stimulation of TNFR1, activation of receptor interacting protein kinase 1 (RIPK1) and caspase 8 promote apoptosis in diverse cell types [19–21]. However, when caspase 8 activity is inhibited genetically or pharmacologically [22–24], RIPK1 signals via receptor interacting protein kinase 3 (RIPK3) and mixed linage kinase domain like pseudokinase (MLKL) to execute necroptosis [15,16,25]. Thus, RIPK1 and caspase 8 function as critical regulators of TNFR1 signaling that can direct either caspase-dependent apoptosis or RIPK3-mediated necroptosis depending on caspase activation state (Figure 1A) [26]. Interestingly, β-cell specific caspase 8 knockout mice display hyperglycemia and loss of islet area with age [27], and caspase 8 mutations have been linked to hyperglycemia in humans [28]. However, the roles of RIPK1 and RIPK3 in TNFα-induced β-cell loss have not been clearly described.

We hypothesized that β cells are susceptible to TNFα-induced cell death and that RIPK1 and RIPK3 regulate this process in concert with caspase activity. To test this hypothesis, we quantified TNFα-induced cell death and caspase activity in immortalized NIT-1 and INS-1 β-cell lines and primary mouse islet cells *in vitro*. We utilized real-time, high-content measurements of cell death, Ripk1 and Ripk3 deficient β cells, a synthetic pan-caspase inhibitor (zVAD-fmk), a small molecule RIPK3 inhibitor (GSK'872), RIPK3 overexpressing β cells, and Ripk3$^{-/-}$ islets to characterize the roles of RIPK1 and RIPK3 in TNFα-induced β-cell loss. We also evaluated the susceptibility of Ripk3$^{-/-}$ mice to hyperglycemia following exposure to the β-cell toxin streptozotocin (STZ). To our knowledge, this study is the first to systematically evaluate the roles of RIPK1, RIPK3, and caspase activity in TNFα-induced β-cell death, and to determine the susceptibility of β cells to caspase-independent programmed cell death.

2. MATERIALS AND METHODS

2.1. Animals and islet isolations

Mice used in this study were obtained from Jackson Laboratories (Bar Harbor, ME) and maintained with ad libitum access to food and water under protocols approved by the Indiana University Institutional Animal Care and Use Committee or the VA Puget Sound Health Care System Institutional Animal Care and Use Committee. Whole body Ripk3 mutant mice (Ripk3$^{-/-}$) were maintained as heterozygotes on a C57BL/6J;DBA/2J background with wild type littermates used as controls. Islets were isolated from 8 to 12-week-old male and female mice by the Indiana University Center for Diabetes and Metabolic Diseases Islet and Physiology Core (IU CDMD), hand-picked, and allowed to recover overnight in RPMI 1640 media with 11.1 mM glucose, 10% fetal bovine serum (FBS), 1% sodium pyruvate and 1% penicillin-streptomycin prior to experimentation.

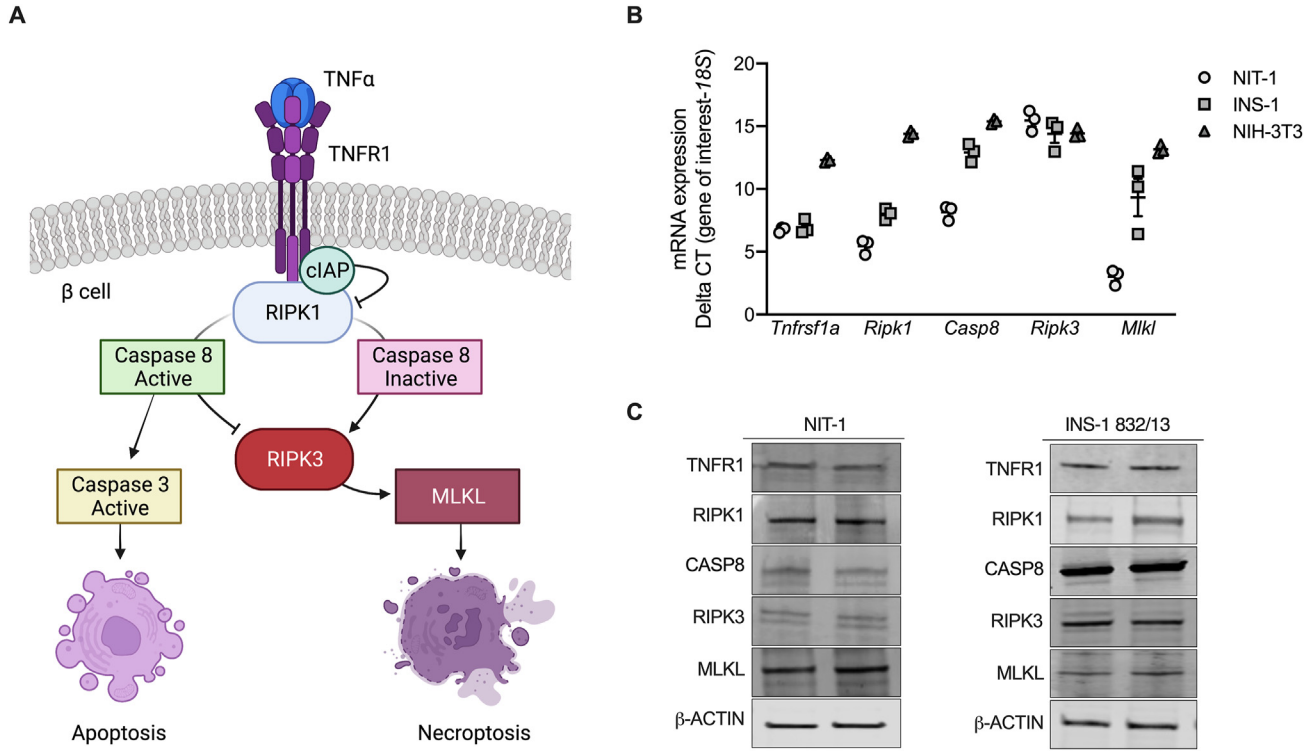

Figure 1: NIT-1 and INS-1 β cells express components of TNFα pathway signaling. A) Schematic of TNFα death signaling pathways as described in non-islet cell types. **B)** *Tnfrsf1a*, *Ripk1*, *Casp8*, *Ripk3* and *Mlkl* RNA expression were quantified in NIT-1 (circles), INS-1 (squares), and NIH-3T3 (triangles) cells, normalized to *18S* rRNA levels, and expressed as ΔCT of the gene of interest (n = 3). **C)** NIT-1 and INS-1 β cells express TNFR1, RIPK1, CASP8, RIPK3 and MLKL protein, as visualized by duplicate immunoblot analysis of 20 μg of protein from total cell lysates.

2.2. Cell lines and culture

INS-1 832/13 cells were obtained from the IU CDMD and the University of Washington Diabetes Research Center Metabolic and Cellular Phenotyping Core (UW DRC). NIT-1 cells were obtained from Dr. Erica Cai (Indiana Biosciences Research Institute). NIH-3T3 cells were obtained from Dr. Michael Kalwat (Indiana Biosciences Research Institute). INS-1 and islet cells were cultured in 11.1 mM glucose RPMI 1640 media while NIT-1 and NIH-3T3 cells were cultured in 25 mM DMEM plus 10% FBS, 1% sodium pyruvate and 1% penicillin-streptomycin in a 37 °C incubator with 5% CO_2. RIPK3 overexpressing INS-1 cell lines were generated via transfection with empty pcDNA3 or pcDNA3 expressing mouse Ripk3 (pcDNA3-mRIPK3), followed by selection with G418 (10131027, ThermoFisher). Ripk1-deficient NIT-1 cells (NIT-1 RIPK1Δ) were generated as previously described [29] using guide RNAs (gRNAs) targeting exons 2–3 of the Ripk1 gene (5'-GAGAAGACAGACCTAGACAG-3' and 5'- CCAAATGG-TCTGATAGATAT-3', Supplemental Figs. 1A and B). Ripk3-deficient NIT-1 cells (NIT-1 RIPK3Δ) were generated using gRNAs targeting exon 6 of the Ripk3 gene (5'-ATGTTATCCCCCAACTCCAG-3' and 5'-GGAGTCTCAGGGCTACCTGG-3', Supplemental Figs. 1C and D). Non-targeting control gRNA (5′-TAAAAACGCTGGCGGCCTAG-3′) was used to generate NIT-1 control cells (NIT-1 CTL). Briefly, lenti-multi-CRISPR plasmid (85402, Addgene, Watertown, MA) was used to express gRNA cassettes, followed by cloning into lentiCRISPR v2 vector (52961, Addgene). Lentivirus containing non-targeting, Ripk1 or Ripk3 gRNA was used to establish NIT-1 CTL, RIPK1Δ and RIPK3Δ cell lines, respectively. Editing of Ripk1 or Ripk3 was verified by PCR of genomic DNA (Supplemental Fig. 1). Mouse islet cells were dispersed in trypsin–EDTA (0.25%, ThermoFisher, Waltham, MA) for 30 min at 37 °C, collected by centrifugation, resuspended in culture media, plated, and allowed to recover prior to analysis. The following reagents were used during cell culture treatment: zVAD-fmk (50 μM, G7232, Promega, Madison, WI), TNFα (40 ng/ml, mouse: CYT-252, Prospec, Rehovot, Israel), BV6 (5 μM, HY-16701, MedChemExpress, Monmouth Junction, NJ), GSK'872 (5 μM, HY-101872, MedChemExpress).

2.3. Quantitative real-time reverse transcription polymerase chain reaction (qRT-PCR)

Total RNA was recovered from NIT-1 cells, INS-1 cells or islets using the RNeasy Mini Kit (74104, Qiagen, Roche, Basel, Switzerland), reverse transcribed with the QuantiTect Reverse Transcription Kit (205411, Qiagen) and subjected to qRT-PCR. Data were normalized to *18S* rRNA levels and expressed as ΔCT of the gene of interest. All qRT-PCR data points represent means of triplicate technical determinations. The following Taqman probes (ThermoFisher Scientific, Waltham, MA) were used to quantify mRNA expression: *Tnfrsf1a* (rat: Rn01492348_m1; mouse: Mm Mm00441883_g1); *Ripk1* (rat: Rn01757369_m1; mouse: Mm00436354_m1); *Casp8* (rat: For: 5'-CCTCTGACCTCCGGTGTTTTA-3', Rev: 5'-ATGTGGTCCAAGCACAGGAA-3', SYBR green chemistry; mouse: Mm00802247_m1); *Ripk3* (Mm00444947_m1); *Mlkl* (rat: Rn01432489_m1, mouse: Mm01244222_m1); and *18S* rRNA (HS99999901_s1).

2.4. Immunoblot analysis

NIT-1, INS-1 and islet cell lysates were prepared in lysis buffer containing 0.1% NP-40, 0.05% deoxycholate, 0.1% SDS, 0.2% sarkosyl, 10% glycerol, 1 mM dithiothreitol, 1 mM EDTA, 10 mM NaF, 50 mM Tris, and protease and phosphatase inhibitors (04693116001 and 0490683700; Millipore Sigma, Burlington, MA). Cell lysates were centrifuged at 10,000 × *g* for 10 min, supernatants collected, and protein concentrations determined by Bradford assay (5000201, BioRad, Hercules, CA). Equal amounts of protein were separated on SDS-PAGE gels (4561093, BioRad) and transferred to PVDF membranes (IPVH00010, Millipore Sigma). Proteins were visualized using the following primary antibodies: TNFR1 (1:1000, ab19139, Abcam, Cambridge, UK); RIPK1 (1:2000, 610458, BD Biosciences, Franklin Lakes, NJ); CASP8 (1:2000, NBP2-80097, Novus Biologicals, Littleton, CO); RIPK3 (1:1000, ab62344, Abcam); MLKL (1:2000. ab243142, Abcam); β-ACTIN (1:2000, ab8226, Abcam). Primary antibodies were detected with goat anti-mouse 800 (1:5000, 926–32210), goat anti-rat 800 (1:5000, 926–32219), or donkey anti-rabbit 680 (1:5000, 926–68071) IRDye secondary antibodies (LI-COR, Lincoln, NE), and visualized with a LI-COR CLx imaging system (LI-COR). Representative immunoblot images are shown.

2.5. Cell death assays

Cell death assays were conducted using Sartorius IncuCyte S3 live-cell imaging and analysis instruments (Sartorius, Göttingen, Germany). Briefly, NIT-1, INS-1, or dispersed islet cells were plated as described and cell culture media containing the treatments of interest and Sytox green (100 nM, S7020, ThermoFisher Scientific, Waltham, MA), a membrane impermeable DNA-binding dye known to label late apoptotic and necroptotic cells [30–32], was added to cells immediately prior to each experiment. Four images from each well were collected with a 10X objective each hour, and cell death was quantified as the average number of Sytox positive fluorescent objects (excitation: 488 nm; emission: 523 nm) at each time point. For comparison within a cell line, changes to cell death were expressed relative to cell death at time t = 0 within each condition and replicate. For experiments comparing distinct cell lines, changes to cell death were expressed as Sytox positive objects per μm^2 phase positive cell area. Percent cell death was quantified using the Sartorius IncuCyte S3 advanced label-free classification analysis software module. Following training on NIT-1 and INS-1 cell populations, label-free analysis of cell morphology was performed using artificial intelligence and multivariate data analytics to identify, classify and quantify live and dead cells [33].

2.6. Caspase activity and DNA laddering assays

Caspase activity assays were conducted on NIT-1 cells, INS-1 cells, or dispersed mouse islet cells. Cells were cultured in 96-well plates and treated for the indicated times, then a luminogenic caspase substrate specific for caspase 3 and caspase 7 (G8090, Promega, Madison, WI) was added for 1 h and luminescence was quantified using a microplate reader (BioTek Synergy H1, Agilent, Santa Clara, CA). DNA laddering assays were conducted on NIT-1 CTL cells following culture in 6-well plates and treatment for the indicated times as previously described [34]. Briefly, cells were lysed and proteins were removed using phenol-chloroform-isoamyl alcohol, then genomic DNA was precipitated from solution with isopropanol, spun at 14k g for 10 min, then resuspended in water. 4 μg of DNA per condition was loaded on 1.5% agarose gels and visualized using ethidium bromide.

2.7. RNAseq analysis

RNAseq was performed at the Indiana University School of Medicine Center for Medical Genomics as described previously [35]. Briefly, RNA was isolated from INS-1 cells with the RNeasy Mini Kit (74104, Qiagen), then used to prepare cDNA libraries with the KAPA mRNA HyperPrep kit (08098093702, Roche, Indianapolis, IN). Libraries were sequenced with a 100 bp paired-end configuration using a NovaSeq 6000 Sequencing System (Illumina, San Diego, CA). Sequence reads were mapped to the reference genome using the STAR (Spliced Transcripts Alignment to a Reference) RNAseq aligner [36]. Differential

gene expression analysis was performed with edgeR [37]. Statistical information is described below.

2.8. Immunoprecipitation

INS-1 cells overexpressing RIPK3 were grown in T75 flasks, treated with TNFα+zVAD for 24 h, and lysed in buffer containing 20 mM Tris HCl, 137 mM NaCl, 1% Nonidet P-40 (NP-40) and 2 mM EDTA. Protein concentrations from each sample were determined by Bradford assay (5000201, BioRad) and 2.5% of the protein lysate was saved as input. Protein A/G coupled Sepharose beads (ab193262, Abcam) were washed with lysis buffer, then equal amounts of protein were incubated with protein A/G beads and either anti-IgG (ab124055, Abcam), anti-RIPK3 (ab62344, Abcam) or anti-MLKL (ab243142, Abcam) primary antibodies overnight at 4 °C with shaking. Protein complexes were collected by centrifugation at 8000×*g* for 3 min at 4 °C, washed, and subjected to immunoblot analysis.

2.9. Intraperitoneal glucose tolerance tests, streptozotocin administration and blood glucose measurements

Mice were fasted overnight prior to intraperitoneal glucose tolerance test (IPGTT), then intraperitoneal glucose was administered at a dose of 2 g/kg body weight. Blood glucose was measured using a handheld glucometer (Contour Next, Bayer, Leverkusen, Germany) via tail vein at 0 (before injection of glucose), 10, 20, 30, 60, 90 and 120 min after glucose injection. Mice were subjected to intraperitoneal administration of low dose streptozotocin (STZ, 50 mg/kg body weight) on 5 consecutive days and non-fasting blood glucose was measured via tail vein on days 0, 3, 7, 9, and 14 after starting STZ using a handheld glucometer (Contour Next, Bayer).

2.10. Statistical analyses

Two-tailed Student's t-tests were used to analyze data sets with two groups, and one-way analysis of variance (ANOVA) was used to analyze data sets with more than two groups. Significant ANOVA results were followed with Sidák post-test to analyze differences between groups of interest and correct for multiple comparisons. Statistical tests were performed with GraphPad Prism 9 software (GraphPad, San Diego, CA). Data are presented as mean ± standard error. A value of $p < 0.05$ was considered significant. Statistical analysis was performed on RNAseq datasets to detect differentially expressed genes (DEGs) using edgeR [37] and negative binomial generalized linear models with likelihood ratio tests. DEGs were identified at $p < 0.05$ and classified as upregulated or downregulated based on log fold change. The p values were corrected for false discovery rate using the Benjamini-Hochberg method, with corrected $p < 0.05$ considered significant.

3. RESULTS

3.1. NIT-1 and INS-1 β cells express components of TNFα pathway signaling and are susceptible to RIPK1- and cIAP-mediated TNFα-induced cell death

TNFα is known to elicit apoptosis and necroptosis via RIPK1 and RIPK3 in non-islet cell types [21,38–41], but these signaling pathways have not been well characterized in β cells (Figure 1A). Like necroptosis-prone NIH-3T3 cells [42], mouse NIT-1 and rat INS-1 β-cell lines express TNF pathway signaling components including TNFR1, RIPK1, CASP8, RIPK3 and MLKL at the mRNA and protein levels (Figure 1B,C). We first generated NIT-1 control (NIT-1 CTL) and NIT-1 RIPK1 deficient cells (NIT-1 RIPK1Δ) containing a 1262 base pair deletion extending from exon 2 to exon 3 of the Ripk1 gene (Supplemental Figs. 1A and B). Using a high-content live-cell imaging and analysis system, we quantified NIT-1 and INS-1 cell death in response to TNFα in real-time each hour. We found that TNFα (shown in blue) significantly increased death in NIT-1 control cells (NIT-1 CTL, shown in circles, Figure 2A,B,C) after 24 h, and that RIPK1 deficient NIT-1 cells (NIT-1 RIPK1Δ, shown in triangles) were protected from TNFα-induced death (Figure 2A,B). Similarly, TNFα treatment increased caspase 3/7 activity in NIT-1 CTL cells, and this was abrogated in NIT-1 RIPK1Δ cells (Figure 2D). Cellular inhibitor of apoptosis proteins (cIAPs) are endogenous inhibitors of cell death that interact with TNF receptor signaling molecules [43]. Treatment with BV6, a small molecule cIAP inhibitor and second mitochondria-derived activator of caspases (SMAC) mimetic [44,45], significantly increased TNFα-induced NIT-1 cell death after 4 h (Figure 2E,F,G), and this effect was diminished in NIT-1 RIPK1Δ cells (Figure 2E,F). The reduced cell death observed in NIT-1 RIPK1Δ versus CTL cells following TNFα- or TNFα+BV6-treatment was associated with reduced caspase 3/7 activity (Figure 2H). Following treatment of NIT-1 CTL cells with TNFα+BV6 for 4 h, we also identified genomic DNA laddering (Figure 2I) characteristic of apoptosis [34]. INS-1 cells were also observed to be susceptible to TNFα-induced cell death which was amplified by BV6 cotreatment (Figure 2J,K,L). Representative cell death images are shown in Figure 2M. These data show that NIT-1 and INS-1 β cells are susceptible to TNFα-induced cell death which is regulated by cIAPs and RIPK1, and that this process occurs in association with increased caspase 3/7 activity.

3.2. NIT-1 and INS-1 β cells are susceptible to TNFα-induced cell death when caspases are inhibited

We next utilized the synthetic pan-caspase inhibitor zVAD-fmk (zVAD) to determine whether increased caspase activity is required for TNFα-induced β-cell death. TNFα treatment strongly induced NIT-1 cell death after 48 h, and cell death was unaltered by zVAD alone (Figure 3A,B,C). TNFα+zVAD treatment (shown in green) significantly increased NIT-1 cell death after 48 h, although to a lesser extent than TNFα alone (shown in blue) (Figure 3A,B,C). As expected, TNFα-induced cell death was associated with increased caspase 3/7 activity, while zVAD or TNFα+zVAD treatment significantly reduced caspase 3/7 activity (Figure 3D). In INS-1 cells, we again found that either TNFα alone or TNFα+zVAD treatment increased cell death, although the magnitude was less than that observed in NIT-1 cells (Figure 3E,F,G). TNFα-induced INS-1 cell death occurred with increased caspase 3/7 activity, and TNFα+zVAD-induced cell death occurred with decreased caspase 3/7 activity (Figure 3H). Representative cell death images are shown in Figure 3I. These data indicate that caspase activation is not required for TNFα-induced cell death in NIT-1 or INS-1 β-cells.

We next determined whether distinct gene expression profiles accompany cell death induced by TNFα versus TNFα+zVAD. Using RNA sequencing of INS-1 cell lysates, we identified genes with high differential expression in response to TNFα or TNFα+zVAD versus vehicle treatment (Figure 3J), with focus on genes expressed differentially between TNFα and TNFα+zVAD conditions. 2932 genes were down-regulated commonly by TNFα or TNFα+zVAD treatment, with 1558 genes down-regulated specifically by TNFα, and 2188 down-regulated specifically by TNFα+zVAD treatment (Figure 3J,K). 301 genes were up-regulated commonly by TNFα and TNFα+zVAD treatment, including *Nfkb2* (nuclear factor kappa B subunit 2) and its transcriptional target *Birc3* (baculoviral IAP Repeat containing 3, also known as cIAP2) (Figure 3J,K). 435 genes were up-regulated specifically by TNFα, while 225 were up-regulated specifically by TNFα+zVAD treatment (Figure 3J,K). Among the genes up-regulated

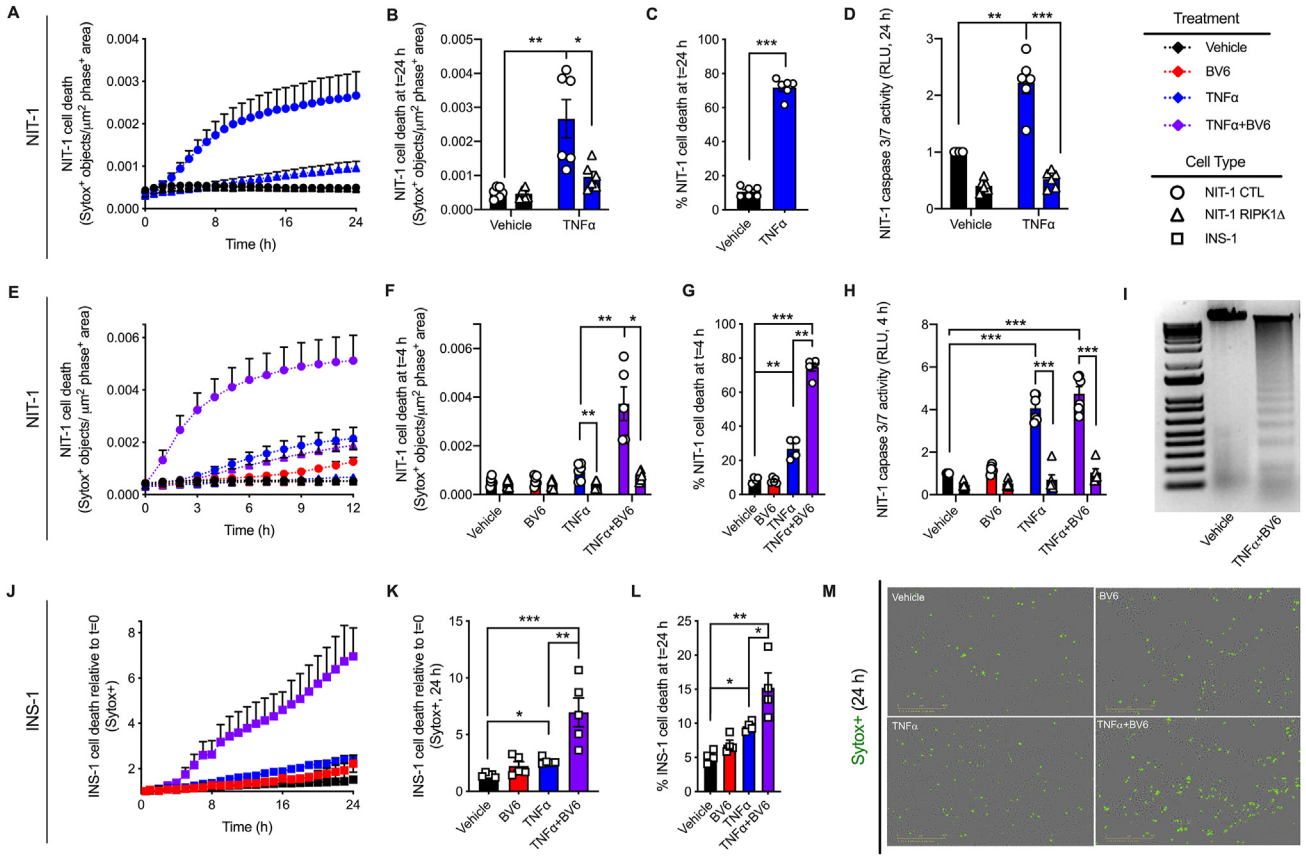

Figure 2: NIT-1 and INS-1 β cells are susceptible to RIPK1- and cIAP-mediated TNFα-induced cell death. A Sartorius IncuCyte S3 live cell imaging and analysis instrument was used to monitor cell death via quantification of Sytox green positive cells. Cell culture treatment conditions are indicated by color (black: vehicle, blue: 40 ng/mL TNFα, red: 5 μM BV6, purple: TNFα+BV6) and β-cell lines are indicated by shapes (NIT-1 CTL: circles, NIT-1 RIPK1Δ: triangles, INS-1: squares). **A)** Cell death was monitored for 24 h in NIT-1 CTL and NIT-1 RIPK1Δ cells following TNFα treatment, and **B)** cell death was quantified 24 h post treatment (n = 6). **C)** Percent NIT-1 CTL cell death was quantified 24 h after treatment with vehicle or TNFα using the Sartorius IncuCyte S3 advanced label-free classification analysis software module, as described (n = 6). **D)** NIT-1 CTL and NIT-1 RIPK1Δ cell caspase 3/7 activity was quantified 24 h after treatment and expressed relative to vehicle treated NIT-1 CTL cells (n = 6). **E)** NIT-1 CTL and NIT-1 RIPK1Δ cells were treated with BV6, TNFα or a combination thereof, then **F)** cell death was quantified 4 h post treatment (n = 5–6). For comparisons between cell lines, cell death was reported as Sytox green positive cell objects normalized to phase positive cell area for each time point. **G)** Percent NIT-1 CTL cell death was quantified 4 h after treatment with BV6, TNFα or a combination thereof using the Sartorius IncuCyte S3 advanced label-free classification analysis software module (n = 4–5). **H)** NIT-1 CTL and NIT-1 RIPK1Δ cell caspase 3/7 activity was quantified 4 h after treatment and expressed relative to vehicle treated NIT-1 CTL cells (n = 4–6). **I)** Genomic DNA was isolated from NIT-1 CTL cells following treatment with vehicle or TNFα+BV6 for 4 h, then visualized on an agarose gel. **J)** For INS-1 cells, cell death was monitored for 24 h following treatment with BV6, TNFα or a combination thereof, then **K)** cell death was quantified 24 h post treatment (n = 5). For comparisons within a cell line, cell death was reported as Sytox green positive cell objects relative to time t = 0. **L)** Percent INS-1 cell death was quantified 24 h after treatment using the Sartorius IncuCyte S3 advanced label-free classification analysis software module, as described (n = 4). **M)** Representative IncuCyte images illustrate Sytox green positive INS-1 cells 24 h post treatment. Data are presented as mean ± SEM and were analyzed by one-way ANOVA followed by Sidák post-test and multiple comparisons correction. $*p < 0.05$; $**p < 0.01$; $***p < 0.001$ as indicated. (For interpretation of the references to color in this figure legend, the reader is referred to the Web version of this article.)

specifically by TNFα+zVAD are lymphocyte expansion molecule (*Lexm*) and lymphocyte activation gene 3 (*Lag3*). These data show that distinct transcriptional profiles characterize TNFα-versus TNFα+z-VAD-induced cell death in INS-1 cells.

3.3. RIPK1 and cIAPs regulate TNFα-induced NIT-1 and INS-1 β-cell death when caspases are inhibited

To examine whether caspase-independent TNFα-induced β-cell death is regulated downstream of TNF receptor signaling, we next treated NIT-1 CTL and RIPK1Δ cells with TNFα+zVAD (shown in green) or TNFα+BV6+zVAD (shown in white). TNFα+zVAD treatment significantly increased NIT-1 cell death over 48 h (Figure 4A,B,C), and this caspase-independent cell death was reduced in RIPK1Δ cells (Figure 4A,B). Cell death in response to TNFα+zVAD was strongly amplified by addition of BV6 (Figure 4A,B,C), and this effect was again abrogated in NIT-1 RIPK1Δ cells (Figure 4A,B). The increased cell death observed with TNFα+zVAD or TNFα+BV6+zVAD treatment occurred when caspase 3/7 activity was significantly reduced compared to vehicle-treated control cells (Figure 4D), and in the absence of genomic DNA laddering (Figure 4E). As in NIT-1 cells, we found that INS-1 cells are susceptible to TNFα+zVAD-induced cell death that is amplified by BV6 co-treatment (Figure 4F,G,H). Representative cell death images are shown in Figure 4I. These data indicate that caspase-independent TNFα-induced NIT-1 and INS-1 cell death is regulated by RIPK1 and cIAPs.

3.4. RIPK3 promotes TNFα-induced INS-1 cell death when caspases are inhibited

RIPK3 has been shown to promote TNFα-induced cell death when caspase activity is inhibited in several cell types [15,25,46]. To

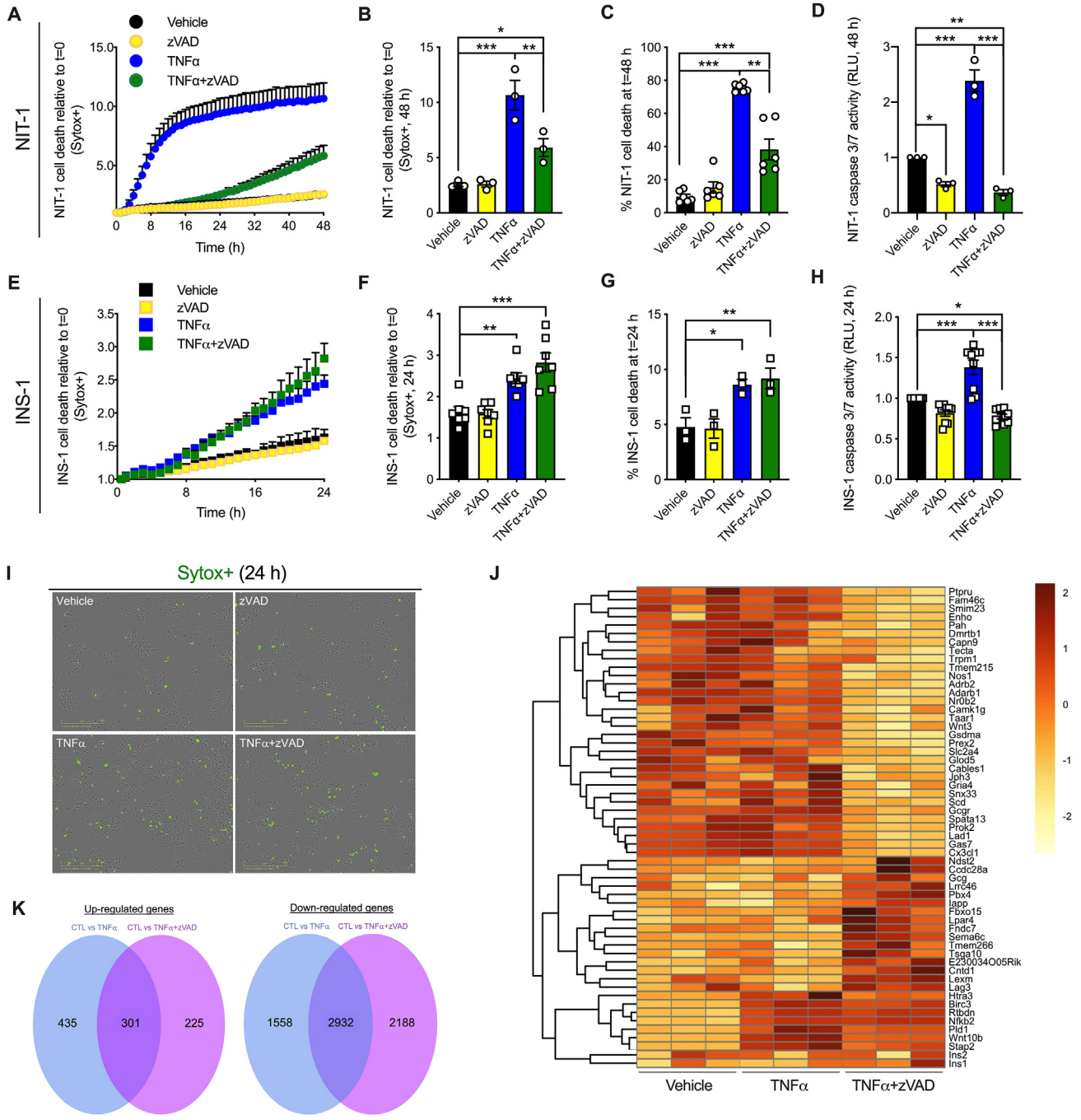

Figure 3: NIT-1 and INS-1 β cells are susceptible to TNFα-induced cell death when caspases are inhibited. A) NIT-1 CTL cell death was monitored over 48 h as described, and **B)** quantified at 48 h post treatment (n = 3). Cell culture treatment conditions are indicated by color (black: vehicle, yellow: 50 μM zVAD, blue: 40 ng/mL TNFα, green: TNFα+zVAD) and β-cell lines are indicated by shapes (NIT-1 CTL: circles, INS-1: squares). **C)** Percent NIT-1 CTL cell death was quantified 48 h after treatment with zVAD, TNFα or a combination thereof using the Sartorius IncuCyte S3 advanced label-free classification analysis software module (n = 6). **D)** NIT-1 CTL cell caspase 3/7 activity was quantified 48 h post treatment and expressed relative to vehicle treated cells (n = 3). **E)** INS-1 cell death was monitored over 24 h, and **F)** quantified at 24 h post treatment (n = 7). **G)** Percent INS-1 cell death was quantified 24 h after treatment using the Sartorius IncuCyte S3 advanced label-free classification analysis software module, as described (n = 3). **H)** INS-1 cell caspase 3/7 activity was quantified 24 h post treatment and expressed relative to vehicle treated cells (n = 9). **I)** Representative IncuCyte images illustrate Sytox green positive INS-1 cells 24 h post treatment. **J)** Heatmap displaying genes with significantly different expression among groups. High expression is shown in dark red and low expression in light yellow (n = 3). **K)** Venn diagrams displaying (left) the number of genes up-regulated commonly by TNFα and TNFα+zVAD (301), up-regulated specifically by TNFα (435), or up-regulated specifically by TNFα+zVAD (225), and (right) the number of genes down-regulated commonly by TNFα and TNFα+zVAD (2932), down-regulated specifically by TNFα (1558), or down-regulated specifically by TNFα+zVAD (2188). **A-H)** Data are presented as mean ± SEM and were analyzed by one-way ANOVA followed by Sidák post-test and multiple comparisons correction. $*p < 0.05$; $**p < 0.01$; $***p < 0.001$ as indicated. **J,K)** Differentially expressed genes were identified at $p < 0.05$, p-values were corrected for false discovery rate using the Benjamini-Hochberg method, and corrected $p < 0.05$ was used to identify significantly different gene expression. (For interpretation of the references to color in this figure legend, the reader is referred to the Web version of this article.)

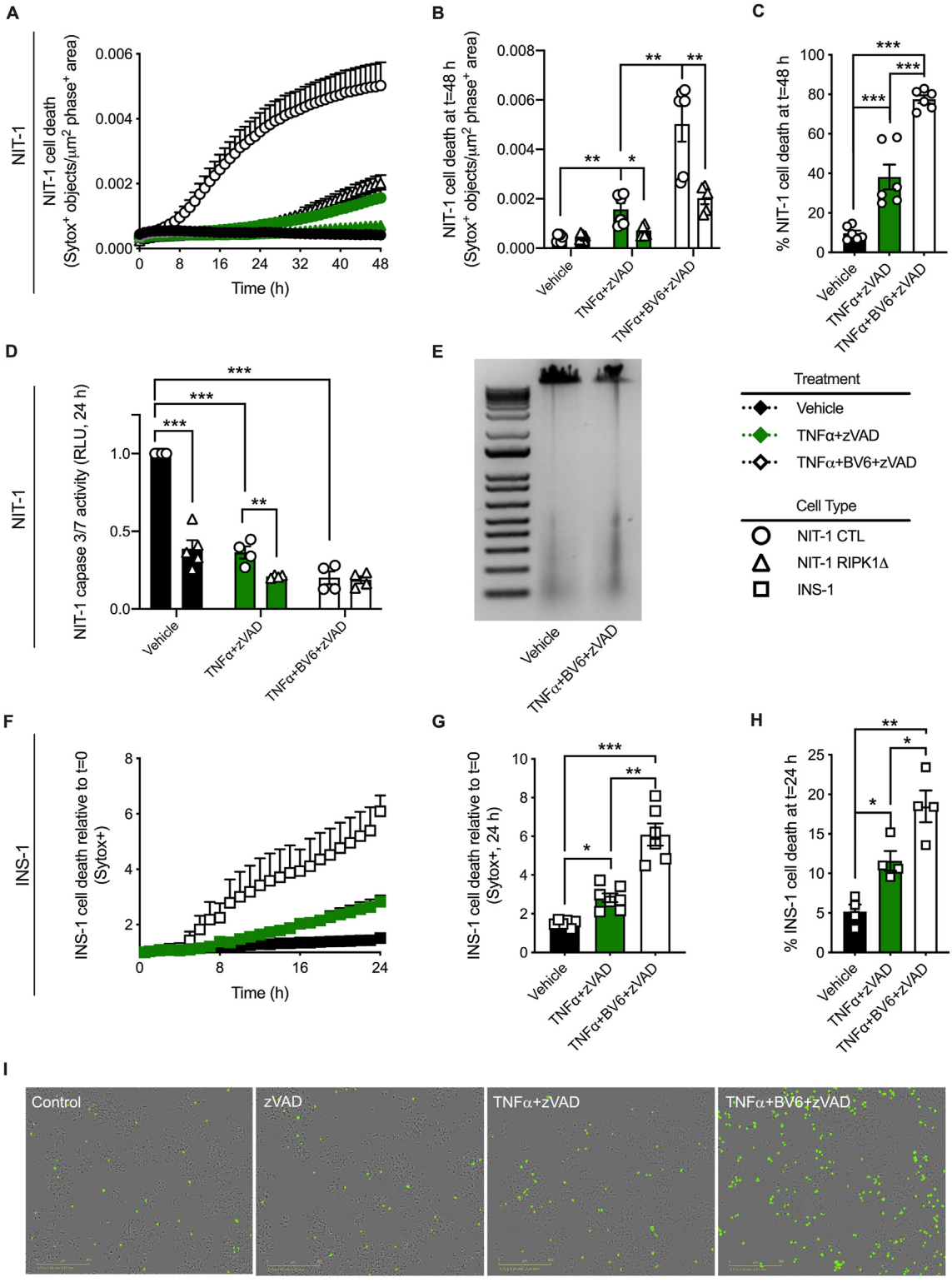

Figure 4: RIPK1 and cIAPs regulate TNFα-induced NIT-1 and INS-1 β-cell death when caspases are inhibited. **A)** NIT-1 CTL and NIT-1 RIPK1Δ cell death was monitored over 48 h, and **B)** quantified at 48 h post treatment (n = 5–6). Cell culture treatment conditions are indicated by color (black: vehicle, green: 40 ng/ml TNFα + 50 μM zVAD, white: TNFα+zVAD + 5 μM BV6) and β-cell lines are indicated by shapes (NIT-1 CTL: circles, NIT-1 RIPK1Δ: triangles, INS-1: squares). **C)** Percent NIT-1 CTL cell death was quantified 48 h after treatment with vehicle, TNFα +zVAD or TNFα+BV6+zVAD using the Sartorius IncuCyte S3 advanced label-free classification analysis software module, as described (n = 6). **D)** NIT-1 CTL and RIPK1Δ cell caspase 3/7 activity was quantified 24 h post treatment and expressed relative to vehicle treated NIT-1 CTL cells (n = 4–5). **E)** Genomic DNA was isolated from NIT-1 CTL cells following treatment with vehicle or TNFα+BV6+zVAD for 8 h, then visualized on an agarose gel. **F)** INS-1 cell death was monitored over 24 h, and **G)** quantified at 24 h post treatment (n = 5–6). **H)** Percent INS-1 cell death was quantified 24 h after treatment using the Sartorius IncuCyte S3 advanced label-free classification analysis software module (n = 4). **I)** Representative IncuCyte images illustrate Sytox green positive INS-1 cells 24 h post treatment. Data are presented as mean ± SEM and were analyzed by one-way ANOVA followed by Sidák post-test and multiple comparisons correction. $*p < 0.05$; $**p < 0.01$; $***p < 0.001$ as indicated. (For interpretation of the references to color in this figure legend, the reader is referred to the Web version of this article.)

determine whether RIPK3 plays a role in caspase-independent TNFα-induced β-cell death, we generated NIT-1 RIPK3 deficient cells (NIT-1 RIPK3Δ, shown in diamonds) containing an 80 base pair insertion in exon 6 of the Ripk3 gene (Supplemental Figs. 1C and D). As before, we found that TNFα treatment significantly increased NIT-1 CTL cell death and caspase 3/7 activity (Figure 5A,B). NIT-1 RIPK3Δ cells were also susceptible to TNFα-induced cell death after 48 h, although this cell death and caspase 3/7 activity were reduced compared to NIT-1 CTL cells (Figure 5A,B). In contrast, NIT-1 RIPK3Δ cells were completely protected from TNFα-induced cell death when caspases were inhibited with zVAD (Figure 5A,B), conditions under which NIT-1 CTL cell death was significantly increased. Next, INS-1 cells were treated with TNFα, zVAD or GSK'872 (a small molecule RIPK3 kinase inhibitor) individually or in combination and evaluated over 24 h. We first treated INS-1 cells with increasing doses of GSK'872 and determined that it did not increase cell death at concentrations up to 20 μM (Supplemental Fig. 2A). Treatment with GSK'872 at 5 μM did not alter INS-1 cell death (Figure 5C) or caspase 3/7 activity (Figure 5D) compared to vehicle treated control cells after 24 h. As before, TNFα increased cell death and caspase 3/7 activity (Figure 5C,D), and co-treatment with TNFα+GSK'872 resulted in similar degrees of cell death and caspase 3/7 activity as TNFα alone (Figure 5C,D). In contrast, TNFα+zVAD treatment elicited INS-1 cell death when caspases were inhibited (Figure 5C,D), and addition of GSK'872 (5 μM) under these conditions (TNFα+zVAD + GSK'872) resulted in significantly less cell death than TNFα+zVAD treatment with no difference in caspase 3/7 activity (Figure 5C,D).

We next evaluated INS-1 cells overexpressing RIPK3. Overexpression of RIPK3 in pcDNA3-mRipk3 INS-1 cells was verified at the RNA and protein levels by qRT-PCR and immunoblot analysis (Figure 5E,F). Neither basal (Supplemental Fig. 2B) nor TNFα-induced (Figure 5G) cell death was altered in pcDNA-3-Empty versus pcDNA3-mRipk3 INS-1 cells. However, TNFα+zVAD treatment caused significantly more cell death in RIPK3 overexpressing pcDNA3-mRipk3 cells compared to control pcDNA-3-Empty cells (Figure 5G). Following treatment with TNFα+zVAD, RIPK3 co-immunoprecipitated with MLKL and caspase 8 from RIPK3 overexpressing INS-1 cell lysates (Figure 5H). Likewise, MLKL co-immunoprecipitated with RIPK3 and caspase 8 under these conditions (Figure 5I). These data indicate that TNFα treatment induces β-cell apoptosis that occurs with caspase 3/7 activation. In contrast, TNFα+zVAD treatment induces a form of β-cell death that occurs when caspase activity is inhibited, is mediated by RIPK3 and is associated with formation of RIPK3-MLKL protein complexes.

3.5. Mouse islets cells are susceptible to TNFα-induced cell death when cIAPs or caspases are inhibited

Previous studies have found that TNFα promotes cell death in immortalized β-cell lines [6,7], but that primary islet cells are resistant to TNFα-induced death [47]. We first confirmed that molecular components of TNF receptor signaling including TNFR1, RIPK1, CASP8, RIPK3 and MLKL are expressed in mouse islets at the mRNA and protein levels (Figure 6A,B). Using our real time cell imaging and analysis platform, we confirmed that treatment with TNFα alone (shown in blue) did not significantly increase dispersed mouse islet cell death after 24 h (Figure 6C). However, in line with our NIT-1 and INS-1 cell findings, inhibition of cIAPs with BV6 significantly increased TNFα-induced mouse islet cell death (Figure 6C, shown in purple). Interestingly, TNFα also increased mouse islet cell death when caspase 3/7 activity was inhibited with zVAD (Figure 6C,D, shown in green). Representative mouse islet cell death images are shown in Figure 6E. These data suggest that primary mouse islet cells are susceptible to TNFα-induced cell death under certain conditions such as when cIAPs or caspases are inhibited.

3.6. RIPK3 promotes TNFα-induced mouse islet cell death when caspases are inhibited

We next tested whether RIPK3 contributes to TNFα-induced mouse islet cell death when caspases are inhibited. Like previous experiments in mouse islet cells, TNFα failed to increase cell death after 24 h, while TNFα+zVAD treatment significantly increased islet cell death (Figure 6F, left panel). Addition of the RIPK3 inhibitor GSK'872 significantly reduced mouse islet cell death in response to TNFα+zVAD, but not TNFα alone (Figure 6F, right panel), and caspase 3/7 activity was not significantly altered by GSK'872 treatment (Figure 6G). We next evaluated Ripk3$^{-/-}$ islets, in which we confirmed loss of RIPK3 expression (Figure 6H). Rates of basal cell death were not different between untreated Ripk3$^{+/+}$ and Ripk3$^{-/-}$ islets cells (Figure 6I). In contrast to our findings with Ripk3$^{+/+}$ islet cells, TNFα+zVAD treatment failed to increase cell death in Ripk3$^{-/-}$ islets compared to vehicle-treated cells (Figure 6J,K). These data indicate that TNFα treatment elicits primary mouse islet cell death when caspases are inhibited, and that this form of cell death is mediated by RIPK3.

3.7. Ripk3$^{-/-}$ mice are protected from STZ-induced hyperglycemia *in vivo*

We next characterized glucose homeostasis in Ripk3$^{+/+}$ and Ripk3$^{-/-}$ mice before and after administration of the β-cell toxin streptozotocin (STZ) to evaluate their susceptibility to hyperglycemia *in vivo* (Figure 7A). Prior to multiple low dose STZ treatment, Ripk3$^{+/+}$ and Ripk3$^{-/-}$ mice exhibited similar glucose tolerance, with no difference in blood glucose before or 10, 20, 30, 60, 90 or 120 min after intraperitoneal glucose administration (Figure 7B). In contrast, following 5 days of low dose STZ and a 5-day recovery, Ripk3$^{-/-}$ mice displayed significantly lower blood glucose than Ripk3$^{+/+}$ mice 60, 90 and 120 min after glucose injection (Figure 7C). Non-fasting blood glucose concentrations were also significantly reduced in Ripk3$^{-/-}$ compared to Ripk3$^{+/+}$ mice 7, 9 and 14 days after initiating STZ treatment (data displayed in Figure 7D,E). These data indicate that Ripk3$^{-/-}$ mice are protected from STZ-induced hyperglycemia and glucose intolerance *in vivo*.

4. DISCUSSION

Acquiring a better understanding of the mechanisms that underly β-cell death may lead to new treatments for diabetes, a disease in which β-cell loss results in insufficient insulin release and hyperglycemia [2,48]. TNFα has been recognized as a mediator of β-cell dysfunction and death in T1D for more than two decades [3,4,6,7,10], and recent clinical studies found that treatment with TNFα neutralizing antibodies improves β-cell function in individuals with recently diagnosed T1D [5,12]. Although TNFα has been recognized as a cytotoxin for nearly 50 years [49], the mechanisms by which TNF receptor signaling elicit β-cell death have not been well characterized. In the present study, we applied knowledge from other cell types and utilized state-of-the-art, high-content live cell imaging and analysis techniques to test the hypothesis that RIPK1 and RIPK3 regulate TNFα-induced β-cell death in concert with caspase activity *in vitro*. Using NIT-1, INS-1 and isolated mouse islet cells and applying small molecule inhibitors of cIAPs, caspases and RIPK3, Ripk1 and Ripk3 gene editing, and RIPK3 overexpression and knockout models, we identified roles for RIPK1 and RIPK3 in regulation of TNFα-induced β-cell death and characterized

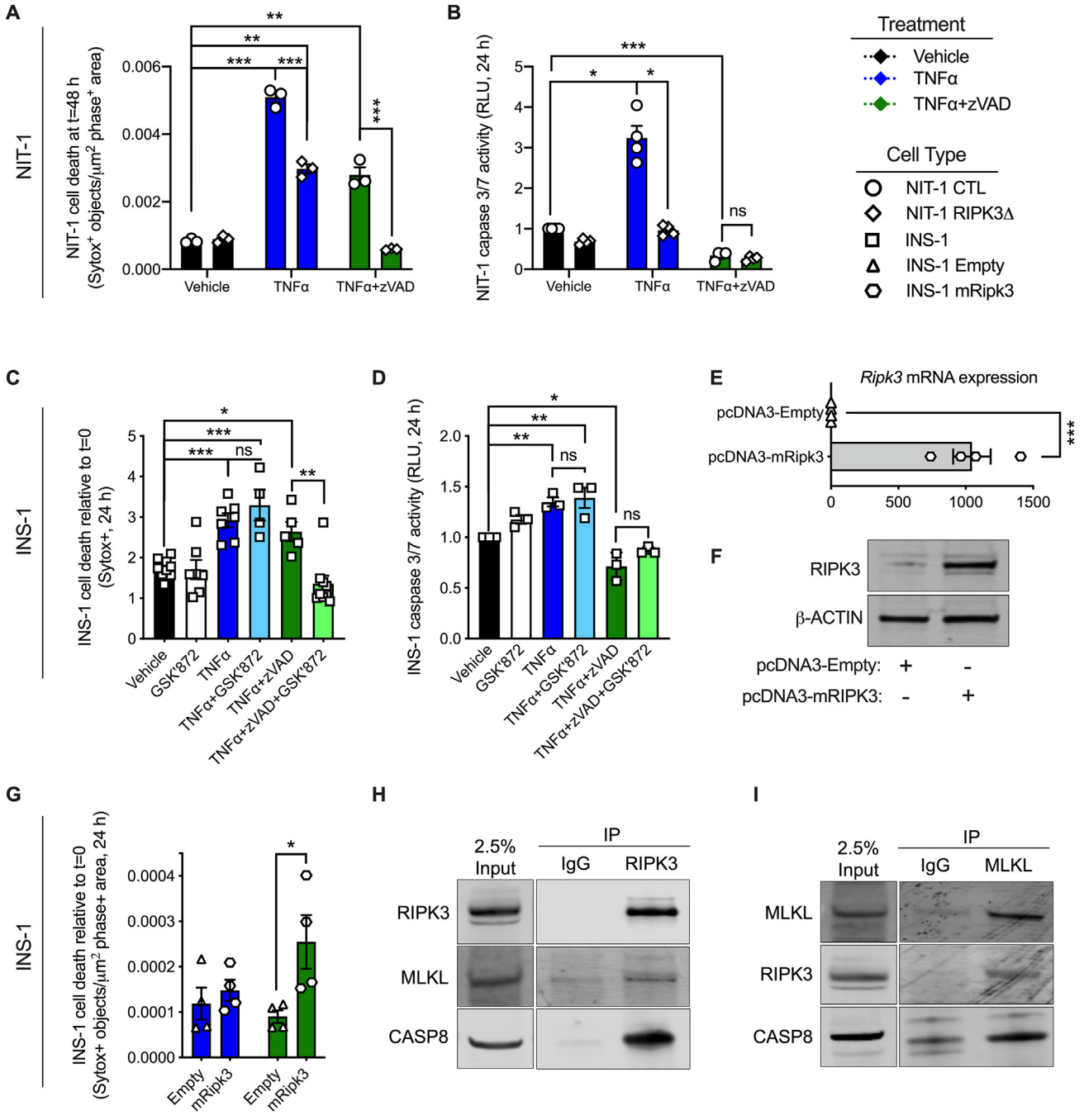

Figure 5: RIPK3 promotes TNFα-induced INS-1 cell death when caspases are inhibited. **A)** NIT-1 CTL and NIT-1 RIPK3Δ cell death was quantified 48 h post treatment (n = 3). Cell culture treatment conditions are indicated by color (black: vehicle, blue: 40 ng/ml TNFα, green: 40 ng/ml TNFα + 50 μM zVAD) and β-cell lines are indicated by shapes (NIT-1 CTL: circles, NIT-1 RIPK3Δ: diamonds, INS-1: squares, INS-1 Empty: triangles, INS-1 mRIPK3: hexagons). **B)** NIT-1 CTL and RIPK3Δ cell caspase 3/7 activity was quantified 24 h post treatment and expressed relative to vehicle treated NIT-1 CTL cells (n = 4). **C)** INS-1 cell death was quantified 24 h post treatment relative to t = 0 (n = 4–9). Cell culture treatment conditions are indicated by color (black: vehicle, white: 5 μM GSK'872, blue: 40 ng/ml TNFα, light blue: TNFα+GSK'872, green: TNFα + 50 μM zVAD, light green: TNFα+zVAD + GSK'872). **D)** INS-1 cell caspase 3/7 activity was quantified 24 h post treatment and expressed relative to vehicle treated cells (n = 3). **E)** *Ripk3* RNA expression (n = 4) and **F)** RIPK3 protein expression were quantified in control (pcDNA3-Empty: triangles) and Ripk3 overexpressing (pcDNA3-mRipk3: hexagons) INS-1 cells. **G)** INS-1 pcDNA3-Empty and pcDNA3-mRipk3 cell death was quantified 24 h post TNFα or TNFα+zVAD treatment (n = 4). **H)** Immunoblot analysis of proteins immunoprecipitated with anti-RIPK3 following 24 h TNFα+zVAD treatment (n = 3). **I)** Immunoblot analysis of proteins immunoprecipitated with anti-MLKL following 24 h TNFα+zVAD treatment (n = 3). Data are presented as mean ± SEM and were analyzed by one-way ANOVA followed by Sidák post-test and multiple comparisons correction. $*p < 0.05$; $**p < 0.01$; $***p < 0.001$; ns, $p > 0.05$ as indicated. (For interpretation of the references to color in this figure legend, the reader is referred to the Web version of this article.)

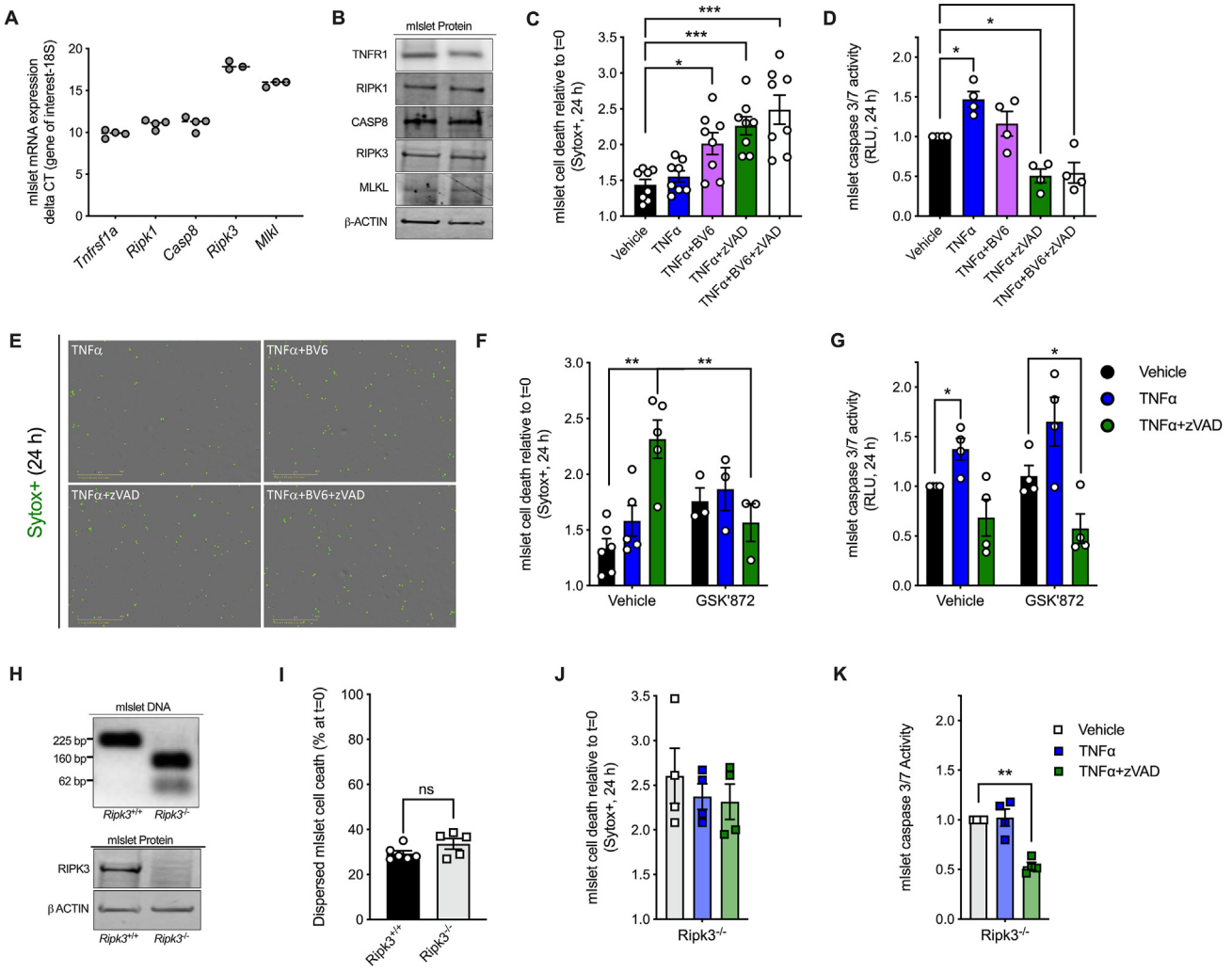

Figure 6: Mouse islets cells are susceptible to TNFα-induced cell death when cIAPs or caspases are inhibited. **A)** Mouse islet cells express components of the TNFα signaling pathway at the RNA and **B)** protein levels. **C)** Mouse islet cell death was quantified 24 h post treatment relative to t = 0 (n = 8). Cell culture treatment conditions are indicated by color (black: vehicle, blue: 40 ng/ml TNFα, purple: TNFα + 5 μM BV6, green: TNFα + 50 μM zVAD, white: TNFα+BV6+zVAD. **D)** Mouse islet cell caspase 3/7 activity was quantified 24 h post treatment and expressed relative to vehicle treated cells (n = 4). **E)** Representative IncuCyte images illustrate Sytox green positive mouse islet cells 24 h post treatment. **F)** Mouse islet cell death was quantified 24 h after treatment with vehicle, TNFα or TNFα+zVAD in the absence (left) or in the presence (right) of the RIPK3 inhibitor GSK'872 (5 μM, n = 3–5). **G)** Mouse islet cell caspase 3/7 activity was quantified 24 h after treatment with vehicle, TNFα or TNFα+zVAD in the absence (left) or in the presence (right) of the RIPK3 inhibitor GSK'872 (n = 4). **H)** Mouse genotyping and islet immunoblot analysis confirmed loss of RIPK3 expression in Ripk3$^{-/-}$ compared to Ripk3$^{+/+}$ mice. **I)** Basal cell death rate was quantified in Ripk3$^{+/+}$ and Ripk3$^{-/-}$ mouse islet cells (n = 5–6). **J)** Ripk3$^{-/-}$ mouse islet cell death was monitored for 24 h and quantified 24 h post treatment relative to t = 0 (n = 4). **K)** Mouse islet cell caspase 3/7 activity was quantified 24 h post treatment and expressed relative to vehicle treated cells (n = 4). Data are presented as mean ± SEM and were analyzed by Student's t-test or one-way ANOVA followed by Sidák post-test and multiple comparisons correction, as described. $*p < 0.05$; $**p < 0.01$; ns, p > 0.05 as indicated. (For interpretation of the references to color in this figure legend, the reader is referred to the Web version of this article.)

factors that modify β-cell susceptibility to TNFα-induced cytotoxicity such as cIAPs, SMAC and caspase activation.

Previous studies have investigated TNFα-induced NFκB activation and FADD signaling in β cells [6,7], but few have evaluated RIPK1, RIPK3 or MLKL [50,51], components of TNF receptor signaling known to promote cell death in other cell types [19,25,52]. Notably, a recent study found that inhibition of RIPK1 promotes porcine islet viability and β-cell abundance [50]. In the present study, we found that NIT-1 RIPK1Δ cells are strongly protected from TNFα-induced cell death (Figure 2A,B,C), that this is associated with reduced caspase 3/7 activation (Figure 2D), and that cIAPs repress TNFα-induced cell death in a RIPK1-dependent manner (Figure 2E,F), a mechanism that has been described in other cell types [53,54].

Since protection of NIT-1 RIPK1Δ cells from TNFα- and BV6-induced cell death was associated with decreased caspase 3/7 activity (Figure 2E–I), we interrogated the role of caspase activation in TNFα-induced β-cell death using zVAD, a small molecule pan-caspase inhibitor. Interestingly, TNFα+zVAD cotreatment significantly increased cell death in NIT-1 (Figure 3B,C) and INS-1 cells (Figure 3F,G), and this cell death occurred in association with reduced caspase 3/7 activity (Figure 3D,H), suggesting a non-apoptotic form of caspase-independent cell death under these conditions. RNA sequencing revealed that a distinct transcriptional profile is present in TNFα+zVAD-compared to TNFα-treated INS-1 cells (Figure 3J,K), consistent with the idea that discrete mechanisms of TNFα-induced β-cell death occur when caspases are active versus inhibited. Interestingly, our RNA sequencing

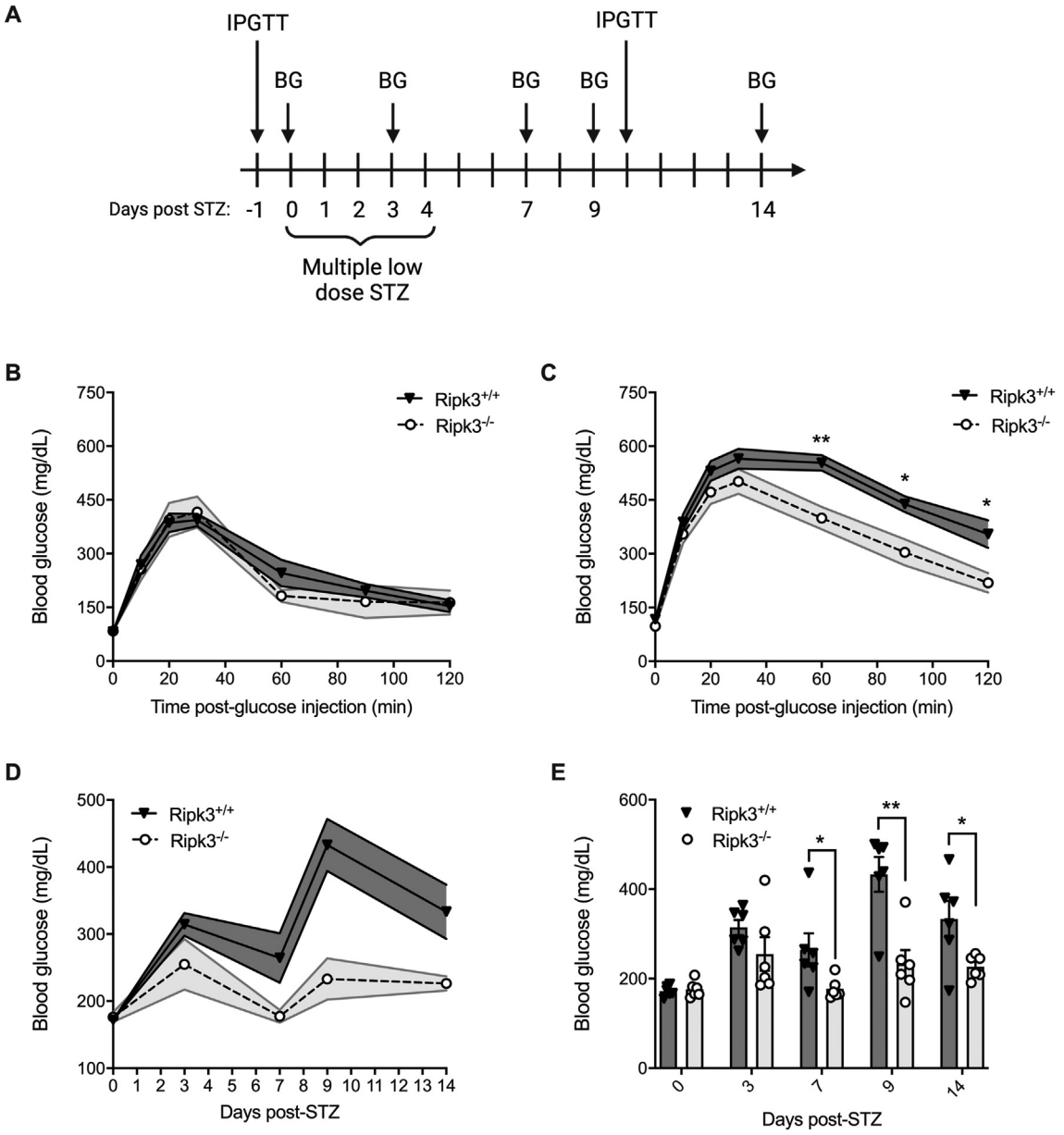

Figure 7: Ripk3$^{-/-}$ mice are protected from STZ-induced hyperglycemia *in vivo*. A) Schematic of multiple low dose-streptozotocin (STZ) treatment and blood glucose monitoring. **B)** Prior to STZ treatment, glucose tolerance was evaluated by intraperitoneal glucose tolerance test (IPGTT) in Ripk3$^{+/+}$ and Ripk3$^{-/-}$ mice (n = 6/group). **C)** 10 days after starting STZ treatment, glucose tolerance was evaluated by IPGTT in Ripk3$^{+/+}$ and Ripk3$^{-/-}$ mice (n = 6/group). **D,E)** Non-fasting blood glucose was quantified in Ripk3$^{+/+}$ and Ripk3$^{-/-}$ mice 0, 3, 7, 9 and 14 days after STZ treatment (n = 6/group), and data are displayed over time **(D)** and at individual time points **(E)**. Data are presented as mean ± SEM and were analyzed by Student's t-test. $*p < 0.05$; $**p < 0.01$; $***p < 0.001$; ns, $p > 0.05$; as indicated.

results identified lymphocyte expansion molecule (*Lexm*) and lymphocyte activation gene 3 (*Lag3*) as genes upregulated specifically by TNFα+zVAD treatment, suggesting that the form of cell death that occurs under these conditions is immune-relevant (Figure 3J). We further characterized this mechanism of caspase-independent β-cell death, observing that it is regulated downstream of TNF receptor signaling by cIAPs and RIPK1. We also observed that *Birc3*, the transcript for cIAP2, is significantly upregulated in response to either TNFα or TNFα+zVAD treatment (Figure 3J), indicating a role for cIAP2 in counter regulation of TNFα-induced β-cell death independent of caspase activity. Indeed, inhibition of cIAPs with BV6 also increased TNFα+zVAD induced cell death in a RIPK1-dependent manner (Figure 4A,B,C), revealing that NIT-1 and INS-1 β cells are susceptible to a caspase-independent mechanism of TNFα-induced cell death that is regulated by cIAPs and RIPK1. Although either TNFα or TNFα+zVAD treatment significantly increased cell death in both NIT-1 and INS-1 cells, we found that the timing and magnitude of this cell death response varied between NIT-1 and INS-1 cells (Figures 2,3). These differences in susceptibility to TNFα- and TNFα+zVAD-induced cell death may be related to variations in expression of TNF receptor signaling components such as caspase 8 and MLKL, which we found to be higher in NIT-1 versus INS-1 cells (Figure 1B).

Previous studies in non-islet cell types have shown that TNFR1 stimulation signals RIPK1 to activate RIPK3 under conditions of caspase inhibition, with RIPK3 then going on to promote necroptosis via MLKL [25,55]. Although apoptosis is widely viewed as the principal mechanism of β-cell death in diabetes [56,57], necroptosis has recently been recognized as a form of programmed cell death that contributes to disease pathogenesis in disorders such as Alzheimer's disease and osteoarthritis [38–40]. Despite potential relevance to the islet inflammation and β-cell autoimmunity observed in T1D, however, non-apoptotic mechanisms of β-cell death have not been well studied [58–60]. Given our finding that β cells are susceptible to caspase-independent cell death, we evaluated the role of RIPK3 in this process. Consistent with the literature, we found that RIPK3 gene editing (Figure 5A,B) or small molecule inhibition of RIPK3 kinase activity (Figure 5C,D) abrogated TNFα-induced β-cell death when caspases were inhibited with zVAD. Moreover, we observed that RIPK3 co-immunoprecipitated with MLKL in RIPK3 overexpressing INS-1 cells following TNFα+zVAD treatment (Figure 5H,I). Notably, we also found that NIT-1 RIPK3Δ cells exhibited reduced caspase 3/7 activation in response to TNFα treatment (Figure 5B), an outcome that did not arise with RIPK3 kinase inhibition in INS-1 cells (Figure 5D). These findings are in line with previous observations linking RIPK3 function with caspase 8 activation and apoptosis [15,61] and suggest that RIPK3 plays an important role in balancing β-cell fate decisions. Together, these data show that RIPK3 promotes TNFα-induced β-cell death when caspases are inhibited, indicative of β cell necroptosis.

In contrast to immortalized β cells [6,7,62], mouse islet cells are known to be resistant to TNFα-induced cell death [6,63], and our studies in mouse islet cells are consistent with these previous findings (Figure 6C,F). However, our studies revealed that small molecule inhibition of either cIAPs (with BV6) or caspases (with zVAD) sensitizes mouse islet cells to TNFα-induced cell death (Figure 6C). Notably, mouse islet cell death induced by TNFα+zVAD treatment was blocked by RIPK3 inhibition with GSK'872 (Figure 6F), and TNFα+zVAD treatment failed to increase cell death and in Ripk3$^{-/-}$ islet cells (Figure 6J). These data show that primary mouse islet cells are also susceptible to TNFα-induced, RIPK3-mediated cell death when caspases are inactivated. Together, our *in vitro* data indicate that therapeutic strategies targeting TNF receptor signaling molecules such as RIPK1 and RIPK3 could promote β-cell survival and improve glucose homeostasis in individuals with T1D.

In these studies, we examined dispersed islet cells to enable use of our high-content live cell imaging and analysis system. We found that these dispersed islet cells exhibited higher rates of basal cell death (Figure 6I) than did NIT-1 or INS-1 cells, and this may have limited the magnitude of primary islet cell death observed in our studies. Still, we identified clear changes in TNFα-induced mouse islet cell death under the conditions tested, and methodological advances may reveal even greater responses in future studies. Some other drawbacks to our islet studies exist. The primary islet cell death measurements reported reflect all islet cell types and are not specific to β cells. Likewise, inhibition of RIPK3 with GSK'872 is expected to impact all islet cell types, and islets from Ripk3$^{-/-}$ mice exhibit knockout in all cell types. Thus, additional studies are needed to characterize the signaling pathways of interest specifically in primary β cells.

To evaluate the role of this signaling pathway in β-cell death *in vivo*, we subjected Ripk3$^{+/+}$ and Ripk3$^{-/-}$ mice to multiple low dose STZ, a β-cell toxin used to model the β-cell loss that occurs in T1D. Although glucose tolerance was not different between Ripk3$^{+/+}$ and Ripk3$^{-/-}$ mice prior to STZ treatment (Figure 7B), Ripk3$^{-/-}$ mice displayed significantly lower blood glucose than Ripk3$^{+/+}$ mice during IPGTTs 10 days after starting STZ (Figure 7C). In addition, Ripk3$^{-/-}$ mice exhibited reduced non-fasting blood glucose 7-, 9-, and 14-days after initiating STZ treatment (Figure 7D,E). Given that STZ selectively kills β cells, we ascribe the reduced hyperglycemia observed in Ripk3$^{-/-}$ mice to a protection from STZ-induced β-cell death. However, it is possible that loss of RIPK3 in tissues outside the islet contributed to the observed phenotype, and additional studies are required to determine whether loss of RIPK3 specifically in β cells improves glucose homeostasis in this model. Likewise, additional studies are needed to understand the roles of β-cell RIPK1 and RIPK3 in diabetogenic β-cell loss *in vivo*. For example, Zhao and colleagues found that loss of RIPK3 failed to protect transplanted islets from T cell-mediated destruction [64], and ER stress was shown to promote RIPK3-dependent IL1β production and NFκB-mediated inflammation in mouse and human islets [51]. Thus, RIPK3 may have additional functions in the islet outside of those studied here. Evaluation of β-cell specific Ripk3 knockout mice would help to clarify the role of RIPK3 in these processes, and use of other models such as NOD mice and kinase dead Ripk1 D138N mice [65] are also needed to establish the relevance of TNFα-mediated β-cell loss in the pathogenesis of diabetes *in vivo*.

It has been hypothesized that β-cell necroptosis could promote islet autoimmunity, inflammation and β-cell loss in T1D [66], but at this time it is not known how caspase inactivation, which promotes RIPK3-mediated cell death *in vitro*, might occur *in vivo*. However, certain viruses inhibit caspase activity [67,68] and there is significant evidence linking viral infection with T1D onset [69,70]. Other factors associated with viral infection such as double stranded viral RNA [71] and IFNγ [72] have also been shown to promote cell death via RIPK1 and RIPK3. Thus, studies to evaluate the relationship between caspase activity, viral responses and mechanisms of β-cell death are warranted. In the current study, we used a synthetic caspase inhibitor (zVAD) to prevent caspase activation. We attribute the ability of zVAD to promote RIPK3-mediated cell death to its inhibition of caspase 8, a molecule of central importance in regulating cell fate. Since zVAD is a pan-caspase inhibitor, however, it is possible that inhibition of caspases other than caspase 8 contributed to our findings. Although we confirmed that zVAD inhibits caspase 8 and caspase 3/7 activation, it is also possible that zVAD has unknown off-target effects. Studies using β-cell specific caspase 8 knockout mice are of interest to further characterize caspase-independent β-cell death.

5. CONCLUSIONS

In conclusion, we found that TNFα can elicit β-cell death in immortalized β-cell lines and dispersed primary mouse islet cells *in vitro*. This process is regulated downstream of TNFR1 by cIAPs, RIPK1, and RIPK3 in concert with caspase activity. Our data indicate that apoptosis is the default mode of β-cell death that occurs downstream of TNFR1 signaling, with this apoptotic cell death being mediated by RIPK1 and increased caspase activity. When caspase activity is inhibited, however, our data show that TNFα signals via RIPK1 and RIPK3 to trigger β-cell necroptosis, an alternative form of caspase-independent cell death. Although additional studies are needed to determine whether necroptosis contributes to β-cell loss and hyperglycemia in the context of T1D, our finding that Ripk3$^{-/-}$ mice are protected from STZ-induced hyperglycemia suggest this is a possibility. Given recent clinical observations that blockade of TNFα signaling promotes glucose homeostasis in individuals with new onset T1D, our studies also position TNFα signaling molecules such as RIPK1 and RIPK3 as potential therapeutic targets to protect β cells in the setting of T1D.

FUNDING

This work was supported in part by funding from the U.S. Department of Veterans Affairs (IK2 BX004659 to ATT, I01 BX001060 to SEK), the National Institutes of Health (R01 CA228098 to AAO, P30 DK097512 to Indiana University Center for Diabetes and Metabolic Diseases, P30 DK017047 to University of Washington Diabetes Research Center, T32 DK064466 to Indiana University Diabetes and Obesity Research Training Program, T32 DK007247 to University of Washington Diabetes, Obesity and Metabolism Training Program), the American Diabetes Association (1-18-PDF-174 to MFH), the Richard L. Roudebush VA Medical Center and the VA Puget Sound Health Care System.

CONTRIBUTION STATEMENT

C.J.C.: Conceptualization, formal analysis, investigation, methodology, writing- original draft, writing-review and editing; N.M., R.C.S.B., L.L., M.F.H., and E.C.: Investigation, methodology, writing-review and editing; A.A.O. and S.E.K.: Conceptualization, methodology, funding acquisition, writing-review and editing; A.T.T.: Conceptualization, data curation, formal analysis, funding acquisition, investigation, methodology, supervision, writing- original draft, writing-review and editing.

DATA AVAILABILITY

Data will be made available on request.

ACKNOWLEDGEMENTS

We thank Travis S. Johnson (Indiana University School of Medicine and Indiana Biosciences Research Institute, Indianapolis, IN) and Rong Qi (Indiana Biosciences Research Institute, Indianapolis, IN) for consultation and assistance with RNAseq data analysis. We thank Emily C. Sims and Matthew J. Repass (Indiana University School of Medicine Angio BioCore) for expert assistance with IncuCyte data collection and analysis. We thank Kara Orr and Lata Udari of the IU CDMD for expert assistance with islet isolation and metabolic phenotyping. We thank Michael Kalwat (Indiana Biosciences Research Institute) for providing NIH-3T3 cells. We acknowledge BioRender for providing the graphic design software used to create the schematic model. Some data from this study were presented at the American Diabetes Association 78th and 81st Scientific Sessions in 2018 and 2021.

CONFLICT OF INTEREST

All authors declare that no competing interests exist.

APPENDIX A. SUPPLEMENTARY DATA

Supplementary data to this article can be found online at https://doi.org/10.1016/j.molmet.2022.101582.

REFERENCES

[1] Mathis, D., Vence, L., Benoist, C., 2001 Dec 13. Beta-cell death during progression to diabetes. Nature 414(6865):792—798.

[2] Meier, J.J., Bhushan, A., Butler, A.E., Rizza, R.A., Butler, P.C., 2005 Nov. Sustained beta cell apoptosis in patients with long-standing type 1 diabetes: indirect evidence for islet regeneration? Diabetologia 48(11):2221—2228.

[3] Green, E.A., Eynon, E.E., Flavell, R.A., 1998 Nov 1. Local expression of TNFα in neonatal NOD mice promotes diabetes by enhancing presentation of islet antigens. Immunity 9(5):733—743.

[4] Kägi, D., Ho, A., Odermatt, B., Zakarian, A., Ohashi, P.S., Mak, T.W., 1999 Apr 15. TNF receptor 1-dependent beta cell toxicity as an effector pathway in autoimmune diabetes. J Immunol 162(8):4598—4605.

[5] Quattrin, T., Haller, M.J., Steck, A.K., Felner, E.I., Li, Y., Xia, Y., et al., 2020 Nov 19. Golimumab and beta-cell function in youth with new-onset type 1 diabetes. N Engl J Med 383(21):2007—2017.

[6] Stephens, L.A., Thomas, H.E., Ming, L., Grell, M., Darwiche, R., Volodin, L., et al., 1999 Jul. Tumor necrosis factor-alpha-activated cell death pathways in NIT-1 insulinoma cells and primary pancreatic beta cells. Endocrinology 140(7):3219—3227.

[7] Chang, I., Kim, S., Kim, J.Y., Cho, N., Kim, Y.H., Kim, H.S., et al., 2003 May 1. Nuclear factor κB protects pancreatic β-cells from tumor necrosis factor-α-mediated apoptosis. Diabetes 52(5):1169—1175.

[8] Kim, H.E., Choi, S.E., Lee, S.J., Lee, J.H., Lee, Y.J., Kang, S.S., et al., 2008 Sep. Tumour necrosis factor-alpha-induced glucose-stimulated insulin secretion inhibition in INS-1 cells is ascribed to a reduction of the glucose-stimulated Ca2+ influx. J Endocrinol 198(3):549—560.

[9] Ortis, F., Pirot, P., Naamane, N., Kreins, A.Y., Rasschaert, J., Moore, F., et al., 2008 Jul. Induction of nuclear factor-kappaB and its downstream genes by TNF-alpha and IL-1beta has a pro-apoptotic role in pancreatic beta cells. Diabetologia 51(7):1213—1225.

[10] Irawaty, W., Kay, T.W.H., Thomas, H.E., 2002 Jan 1. Transmembrane TNF and IFNγ induce caspase-independent death of primary mouse pancreatic beta cells. Autoimmunity 35(6):369—375.

[11] Yang, X.D., Tisch, R., Singer, S.M., Cao, Z.A., Liblau, R.S., Schreiber, R.D., et al., 1994 Sep 1. Effect of tumor necrosis factor alpha on insulin-dependent diabetes mellitus in NOD mice. I. The early development of autoimmunity and the diabetogenic process. J Exp Med 180(3):995—1004.

[12] Mastrandrea, L., Yu, J., Behrens, T., Buchlis, J., Albini, C., Fourtner, S., et al., 2009 Apr 14. Etanercept treatment in children with new-onset type 1 diabetes: pilot randomized, placebo-controlled, double-blind study. Diabetes Care 32(7):1244—1249.

[13] Eizirik, D.L., Mandrup-Poulsen, T., 2001. A choice of death—the signal-transduction of immune-mediated beta-cell apoptosis. Diabetologia 44(12):2115—2133.

[14] Linkermann, A., Green, D.R., 2014 Jan 30. Necroptosis. N Engl J Med. 370(5):455—465.

[15] Newton, K., Dugger, D.L., Wickliffe, K.E., Kapoor, N., Almagro, MC de, Vucic, D., et al., 2014 Mar 21. Activity of protein kinase RIPK3 determines whether cells die by necroptosis or apoptosis. Science 343(6177):1357—1360.

[16] Vandenabeele, P., Galluzzi, L., Vanden Berghe, T., Kroemer, G., 2010 Oct. Molecular mechanisms of necroptosis: an ordered cellular explosion. Nat Rev Mol Cell Biol 11(10):700—714.

[17] Kaczmarek, A., Vandenabeele, P., Krysko, D.V., 2013 Feb 21. Necroptosis: the release of damage-associated molecular patterns and its physiological relevance. Immunity 38(2):209—223.

[18] Murai, S., Yamaguchi, Y., Shirasaki, Y., Yamagishi, M., Shindo, R., Hildebrand, J.M., et al., 2018 Oct 26. A FRET biosensor for necroptosis uncovers two different modes of the release of DAMPs. Nat Commun 9(1):4457.

[19] Wang, J.S., Wu, D., Huang, D.Y., Lin, W.W., 2015 Sep 18. TAK1 inhibition-induced RIP1-dependent apoptosis in murine macrophages relies on constitutive TNF-α signaling and ROS production. J Biomed Sci 22(1):76.

[20] Amin, P., Florez, M., Najafov, A., Pan, H., Geng, J., Ofengeim, D., et al., 2018 Jun 26. Regulation of a distinct activated RIPK1 intermediate bridging complex I and complex II in TNFα-mediated apoptosis. Proc Natl Acad Sci 115(26):E5944—E5953.

[21] Dannappel, M., Vlantis, K., Kumari, S., Polykratis, A., Kim, C., Wachsmuth, L., et al., 2014 Sep. RIPK1 maintains epithelial homeostasis by inhibiting apoptosis and necroptosis. Nature 513(7516):90—94.

[22] Liu, C.Y., Takemasa, A., Liles, W.C., Goodman, R.B., Jonas, M., Rosen, H., et al., 2003 Jan 1. Broad-spectrum caspase inhibition paradoxically augments cell death in TNF-alpha -stimulated neutrophils. Blood 101(1):295—304.
[23] Varfolomeev, E.E., Schuchmann, M., Luria, V., Chiannilkulchai, N., Beckmann, J.S., Mett, I.L., et al., 1998 Aug. Targeted disruption of the mouse Caspase 8 gene ablates cell death induction by the TNF receptors, Fas/Apo1, and DR3 and is lethal prenatally. Immunity 9(2):267—276.
[24] Fritsch, M., Günther, S.D., Schwarzer, R., Albert, M.C., Schorn, F., Werthenbach, J.P., et al., 2019 Nov. Caspase-8 is the molecular switch for apoptosis, necroptosis and pyroptosis. Nature 575(7784):683—687.
[25] Wang, H., Sun, L., Su, L., Rizo, J., Liu, L., Wang, L.F., et al., 2014 Apr 10. Mixed lineage kinase domain-like protein MLKL causes necrotic membrane disruption upon phosphorylation by RIP3. Mol Cell 54(1):133—146.
[26] Tummers, B., Green, D.R., 2017 May. Caspase-8; regulating life and death. Immunol Rev 277(1):76—89.
[27] Liadis, N., Salmena, L., Kwan, E., Tajmir, P., Schroer, S.A., Radziszewska, A., et al., 2007 Sep 1. Distinct in vivo roles of caspase-8 in β-cells in physiological and diabetes models. Diabetes 56(9):2302—2311.
[28] Tabebi, M., Khabou, B., Boukadi, H., Ben Hamad, M., Ben Rhouma, B., Tounsi, S., et al., 2018 Jan 10. Association study of apoptosis gene polymorphisms in mitochondrial diabetes: a potential role in the pathogenicity of MD. Gene 639:18—26.
[29] Cai, E.P., Ishikawa, Y., Zhang, W., Leite, N.C., Li, J., Hou, S., et al., 2020 Sep. Genome-scale in vivo CRISPR screen identifies RNLS as a target for beta cell protection in type 1 diabetes. Nat Metab 2(9):934—945.
[30] Galluzzi, L., Aaronson, S.A., Abrams, J., Alnemri, E.S., Andrews, D.W., Baehrecke, E.H., et al., 2009 Aug. Guidelines for the use and interpretation of assays for monitoring cell death in higher eukaryotes. Cell Death Differ 16(8): 1093—1107.
[31] Wlodkowic, D., Skommer, J., Darzynkiewicz, Z., 2012 Oct. Cytometry of apoptosis. Historical perspective and new advances. Exp Oncol 34(3):255—262.
[32] Grootjans, S., Hassannia, B., Delrue, I., Goossens, V., Wiernicki, B., Dondelinger, Y., et al., 2016 Aug. A real-time fluorometric method for the simultaneous detection of cell death type and rate. Nat Protoc 11(8):1444—1454.
[33] Yamanishi, C., Parigoris, E., Takayama, S., 2020 Sep 22. Kinetic analysis of label-free microscale collagen gel contraction using machine learning-aided image analysis. Front Bioeng Biotechnol 8:582602.
[34] Rahbar Saadat, Y., Saeidi, N., Zununi Vahed, S., Barzegari, A., Barar, J., 2015. An update to DNA ladder assay for apoptosis detection. BioImpacts BI 5(1): 25—28.
[35] Bone, R.N., Oyebamiji, O., Talware, S., Selvaraj, S., Krishnan, P., Syed, F., et al., 2020 Nov. A computational approach for defining a signature of β-cell golgi stress in diabetes. Diabetes 69(11):2364—2376.
[36] Dobin, A., Davis, C.A., Schlesinger, F., Drenkow, J., Zaleski, C., Jha, S., et al., 2013 Jan 1. STAR: ultrafast universal RNA-seq aligner. Bioinformatics 29(1): 15—21.
[37] Robinson, M.D., McCarthy, D.J., Smyth, G.K., 2010 Jan 1. edgeR: a Bioconductor package for differential expression analysis of digital gene expression data. Bioinformatics 26(1):139—140.
[38] Caccamo, A., Branca, C., Piras, I.S., Ferreira, E., Huentelman, M.J., Liang, W.S., et al., 2017 Sep. Necroptosis activation in Alzheimer's disease. Nat Neurosci 20(9):1236—1246.
[39] Wang, S., Zhang, C., Hu, L., Yang, C., 2016 Mar. Necroptosis in acute kidney injury: a shedding light. Cell Death Dis 7(3) e2125—e2125.
[40] Riegger, J., Brenner, R.E., 2019 Sep 17. Evidence of necroptosis in osteoarthritic disease: investigation of blunt mechanical impact as possible trigger in regulated necrosis. Cell Death Dis 10(10):1—12.
[41] Chen, A.Q., Fang, Z., Chen, X.L., Yang, S., Zhou, Y.F., Mao, L., et al., 2019 Jun 20. Microglia-derived TNF-α mediates endothelial necroptosis aggravating blood brain—barrier disruption after ischemic stroke. Cell Death Dis 10(7):1—18.
[42] Orozco, S., Yatim, N., Werner, M.R., Tran, H., Gunja, S.Y., Tait, S.W.G., et al., 2014 Oct. RIPK1 both positively and negatively regulates RIPK3 oligomerization and necroptosis. Cell Death Differ 21(10):1511—1521.
[43] Silke, J., Brink, R., 2010 Jan. Regulation of TNFRSF and innate immune signalling complexes by TRAFs and cIAPs. Cell Death Differ 17(1):35—45.
[44] El-Mesery, M., Shaker, M.E., Elgaml, A., 2016 Dec. The SMAC mimetic BV6 induces cell death and sensitizes different cell lines to TNF-α and TRAIL-induced apoptosis. Exp Biol Med 241(18):2015—2022.
[45] Li, W., Li, B., Giacalone, N.J., Torossian, A., Sun, Y., Niu, K., et al., 2011 Nov 1. BV6, an IAP antagonist, activates apoptosis and enhances radiosensitization of non-small cell lung carcinoma in vitro. J Thorac Oncol 6(11):1801—1809.
[46] Akara-amornthum, P., Lomphithak, T., Choksi, S., Tohtong, R., Jitkaew, S., 2020 Jan 8. Key necroptotic proteins are required for Smac mimetic-mediated sensitization of cholangiocarcinoma cells to TNF-α and chemotherapeutic gemcitabine-induced necroptosis. PLoS ONE 15(1):e0227454.
[47] Soldevila, G., Buscema, M., Doshi, M., James, R.F., Bottazzo, G.F., Pujol-Borrell, R., 1991 Apr. Cytotoxic effect of IFN-gamma plus TNF-alpha on human islet cells. J Autoimmun 4(2):291—306.
[48] Barker, A., Lauria, A., Schloot, N., Hosszufalusi, N., Ludvigsson, J., Mathieu, C., et al., 2014 Mar. Age-dependent decline of β-cell function in type 1 diabetes after diagnosis: a multi-centre longitudinal study. Diabetes Obes Metab 16(3):262—267.
[49] Carswell, E.A., Old, L.J., Kassel, R.L., Green, S., Fiore, N., Williamson, B., 1975 Sep. An endotoxin-induced serum factor that causes necrosis of tumors. Proc Natl Acad Sci U S A 72(9):3666—3670.
[50] Lau, H., Corrales, N., Rodriguez, S., Luong, C., Mohammadi, M., Khosrawipour, V., et al., 2020 Dec 7. Dose-dependent effects of necrostatin-1 supplementation to tissue culture media of young porcine islets. PLoS ONE 15(12):e0243506.
[51] Yang B, Maddison LA, Zaborska KE, Dai C, Yin L, Tang Z, et al. RIPK3-mediated inflammation is a conserved β cell response to ER stress. Sci Adv. 6(51):eabd7272.
[52] Lawlor, K.E., Khan, N., Mildenhall, A., Gerlic, M., Croker, B.A., D'Cruz, A.A., et al., 2015 Feb 18. RIPK3 promotes cell death and NLRP3 inflammasome activation in the absence of MLKL. Nat Commun 6:6282.
[53] Annibaldi, A., Wicky John, S., Vanden Berghe, T., Swatek, K.N., Ruan, J., Liccardi, G., et al., 2018 Feb 15. Ubiquitin-mediated regulation of RIPK1 kinase activity independent of IKK and MK2. Mol Cell 69(4):566—580 e5.
[54] Petersen, S.L., Peyton, M., Minna, J.D., Wang, X., 2010 Jun 29. Overcoming cancer cell resistance to Smac mimetic induced apoptosis by modulating cIAP-2 expression. Proc Natl Acad Sci 107(26):11936—11941.
[55] Cho, Y.S., Challa, S., Moquin, D., Genga, R., Ray, T.D., Guildford, M., et al., 2009 Jun 12. Phosphorylation-driven assembly of the RIP1-RIP3 complex regulates programmed necrosis and virus-induced inflammation. Cell 137(6): 1112—1123.
[56] Jörns, A., Günther, A., Hedrich, H.J., Wedekind, D., Tiedge, M., Lenzen, S., 2005 Jul. Immune cell infiltration, cytokine expression, and beta-cell apoptosis during the development of type 1 diabetes in the spontaneously diabetic LEW.1AR1/Ztm-iddm rat. Diabetes 54(7):2041—2052.
[57] O'Brien, B.A., Harmon, B.V., Cameron, D.P., Allan, D.J., 1997 May. Apoptosis is the mode of beta-cell death responsible for the development of IDDM in the nonobese diabetic (NOD) mouse. Diabetes 46(5):750—757.
[58] Babon, J.A.B., DeNicola, M.E., Blodgett, D.M., Crèvecoeur, I., Buttrick, T.S., Maehr, R., et al., 2016 Dec. Analysis of self-antigen specificity of islet-infiltrating T cells from human donors with type 1 diabetes. Nat Med 22(12):1482—1487.
[59] Eizirik, D.L., Colli, M.L., Ortis, F., 2009 Apr. The role of inflammation in insulitis and beta-cell loss in type 1 diabetes. Nat Rev Endocrinol 5(4): 219—226.

[60] Mukherjee, N., Lin, L., Contreras, C.J., Templin, A.T., 2021 Nov 22. β-Cell death in diabetes: past discoveries, present understanding, and potential future advances. Metabolites 11(11):796.

[61] Mandal, P., Berger, S.B., Pillay, S., Moriwaki, K., Huang, C., Guo, H., et al., 2014 Nov 20. RIP3 induces apoptosis independent of pro-necrotic kinase activity. Mol Cell 56(4):481—495.

[62] Ishizuka, N., Yagui, K., Tokuyama, Y., Yamada, K., Suzuki, Y., Miyazaki, J ichi, et al., 1999 Dec 1. Tumor necrosis factor alpha signaling pathway and apoptosis in pancreatic β cells. Metabolism 48(12):1485—1492.

[63] Barthson, J., Germano, C.M., Moore, F., Maida, A., Drucker, D.J., Marchetti, P., et al., 2011 Nov 11. Cytokines tumor necrosis factor-α and interferon-γ induce pancreatic β-cell apoptosis through STAT1-mediated Bim protein activation. J Biol Chem 286(45):39632—39643.

[64] Zhao, Y., Scott, N.A., Fynch, S., Elkerbout, L., Wong, W.W.L., Mason, K.D., et al., 2015 Jan 1. Autoreactive T cells induce necrosis and not BCL-2-regulated or death receptor-mediated apoptosis or RIPK3-dependent necroptosis of transplanted islets in a mouse model of type 1 diabetes. Diabetologia 58(1):140—148.

[65] Polykratis, A., Hermance, N., Zelic, M., Roderick, J., Kim, C., Van, T.M., et al., 2014 Aug 15. RIPK1 kinase inactive mice are viable and protected from TNF-induced necroptosis in vivo. J Immunol 193(4):1539—1543.

[66] Tonnus, W., Belavgeni, A., Beuschlein, F., Eisenhofer, G., Fassnacht, M., Kroiss, M., et al., 2021 Aug. The role of regulated necrosis in endocrine diseases. Nat Rev Endocrinol 17(8):497—510.

[67] Cheng, E.H., Nicholas, J., Bellows, D.S., Hayward, G.S., Guo, H.G., Reitz, M.S., et al., 1997 Jan 21. A Bcl-2 homolog encoded by Kaposi sarcoma-associated virus, human herpesvirus 8, inhibits apoptosis but does not heterodimerize with Bax or Bak. Proc Natl Acad Sci U S A 94(2):690—694.

[68] Thome, M., Schneider, P., Hofmann, K., Fickenscher, H., Meinl, E., Neipel, F., et al., 1997 Apr 3. Viral FLICE-inhibitory proteins (FLIPs) prevent apoptosis induced by death receptors. Nature 386(6624):517—521.

[69] Filippi, C.M., von Herrath, M.G., 2008 Nov. Viral trigger for type 1 diabetes. Diabetes 57(11):2863—2871.

[70] Takita, M., Jimbo, E., Fukui, T., Aida, K., Shimada, A., Oikawa, Y., et al., 2019 Oct 1. Unique inflammatory changes in exocrine and endocrine pancreas in enterovirus-induced fulminant type 1 diabetes. J Clin Endocrinol Metab 104(10):4282—4294.

[71] Jiao, H., Wachsmuth, L., Kumari, S., Schwarzer, R., Lin, J., Eren, R.O., et al., 2020 Apr. Z-nucleic-acid sensing triggers ZBP1-dependent necroptosis and inflammation. Nature 580(7803):391—395.

[72] Yang, D., Liang, Y., Zhao, S., Ding, Y., Zhuang, Q., Shi, Q., et al., 2020 Apr. ZBP1 mediates interferon-induced necroptosis. Cell Mol Immunol 17(4):356—368.

